AIAA Guidance, Navigation and Control Conference and Exhibit
20 - 23 August 2007, Hilton Head, South Carolina

AIAA 2007-6528

Integration of Adaptive Estimation and Adaptive Control Design for Uncertain Nonlinear Systems

Ramachandra J. Sattigeri [1] and Anthony J. Calise.[2]
Georgia Institute of Technology, Atlanta, GA 30332-0150

Byoung Soo Kim [3]
Gyeongsang National University, Gyeongnam, SOUTH KOREA

This paper presents a method to integrate adaptive estimation and adaptive control designs for a class of uncertain nonlinear systems having both parametric uncertainties and unmodeled dynamics. The method is based on Lyapunov-like stability analysis of all the errors in the closed-loop system. The adaptive estimator considered is a linear, time-varying Kalman filter augmented by the output of an *observer* neural network. The observer neural network compensates the nominal Kalman filter for modeling errors. The estimated states are used in the construction of an adaptive control solution that is based on approximate feedback linearization augmented with the outputs of an adaptive neural network controller. The presented approach is then applied to a vision-based formation flight control problem. The objective is for a follower aircraft to maintain range from a maneuvering leader aircraft using a monocular fixed camera for passive sensing of the leader's relative motion. In the implementation, the states of the adaptive estimator are estimates of line-of-sight variables and the outputs of the observer neural network are estimates of the leader acceleration. The adaptive control solution considered is an integrated guidance and control design that includes online adaptation to unmodeled nonlinearities such as the unknown leader aircraft acceleration and parametric uncertainties in the own-aircraft aerodynamic derivatives. Simulation results using a nonlinear 6DOF simulation model of a fixed-wing UAV are presented to illustrate the feasibility and efficacy of the approach.

I. Introduction

This paper presents a method for integrating adaptive estimation and adaptive control designs for a class of uncertain nonlinear systems having both parametric uncertainties and unmodeled dynamics. The adaptive estimator is a linear time-varying Kalman filter augmented with an observer neural network (NN) that is trained online using the composite adaptation approach presented in Ref. [2]. The estimated states are used in the construction of an adaptive control solution that is based on approximate feedback linearization augmented with the output of controller NN that is also trained online. It is clear that any ad-hoc integration is not sufficient to guarantee the stability of the overall adaptive estimator-controller design, since the certainty equivalence principle does not apply when the adaptive estimator is integrated with the adaptive controller in this fashion. Hence the motivation for this paper is to provide a theoretical justification for the integration of the adaptive estimator and controller solutions based on a Lyapunov-like stability analysis of the closed-loop system errors. It should be noted that similar approaches have been developed and applied to certain types of systems. Ref. [3] constructs an adaptive NN observer providing state estimates to an adaptive NN controller for robotic type systems. The observer NN approximates the state-dependent uncertainty and the NN in the controller approximates a nonlinear function of the tracking error, states of the system and the state estimation error. In this approach, the relative degree of each of the outputs being regulated is two and is a full vector relative degree design [4]. Lyapunov-like stability analysis is used to show Uniform Ultimate Boundedness (UUB) [1] of the system errors. Ref. [5] presents an approach in which an adaptive NN observer is coupled with a backstepping controller for nonlinear systems with uncertainties that are functions only of the output of the system. Similar adaptive observer based controller design approaches are

[1] Graduate Research Assistant, School of Aerospace Engineering, gte334x@mail.gatech.edu, AIAA Member.
[2] Professor, School of Aerospace Engineering, anthony.calise@ae.gatech.edu, Fellow AIAA.
[3] Associate Professor, School of Mechanical and Aerospace Engineering, bskim@gsnu.ac.kr, AIAA Member.

presented in Ref. [6-9] for full relative degree systems. The approach presented in this paper differs from that in Ref. [3, 5-9] in two significant aspects. The approaches in Ref. [3, 5-9] all require knowledge of the dimension of the complete state vector of the system. The approach developed in this paper is applicable to systems with unmodeled dynamics, and does not require knowledge of the dimension of the complete state vector. An adaptive observer is built to estimate only the modeled states of the system. In addition, the approaches in Ref. [3, 5-9] permit augmentation only of a linear time-invariant observer with a NN. In this paper, we consider augmentation of a linear, time-varying observer with a NN. These extensions in theory are important to allow application in certain guidance and flight control applications. For example in applications such as missile intercept guidance, target tracking and vision-based formation flight, not all the states are available for feedback and the target dynamics are the poorly modeled or unmodeled.

The problem of leader-follower formation flight in which the follower aircraft is equipped with only an onboard camera to track the leader aircraft is quite challenging. This problem requires simultaneous sensor data processing, state estimation and tracking control in the presence of unmodeled disturbances (leader acceleration) and measurement uncertainties. Sensor data processing involves fast converging image processing algorithms that track the leader aircraft in the presence of background clutter and derive noisy measurements of the leader aircraft's position relative to itself [10,11]. A consequence of using a monocular fixed camera is that the range is not available as a measurement. So the measurements from the image processing algorithm are fed into a nonlinear filter, e.g., an Extended Kalman Filter (EKF), which computes estimates of range and other line-of-sight (LOS) variables that are required in the guidance and control algorithms [10].

In a previous paper [12], we presented an adaptive approach to an integrated guidance and control (IGC) design for a LOS based formation flight configuration of a leader and a follower aircraft. The formation flight objective was for the follower aircraft to regulate range and bearing angle rates to specified values from a maneuvering leader aircraft. The IGC solution includes online adaptation to unmodeled nonlinearities such as the unknown target (leader aircraft) acceleration and parametric uncertainties in the aircraft aerodynamic derivatives. There are important reasons for pursuing an IGC design. IGC designs have been cited in literature as a way of overcoming the shortcomings of conventional guidance and flight control designs that rely on the time-scale separation assumption between the guidance and autopilot subsystems [13-16]. In the case of missile intercept guidance, it has been stated that an IGC formulation can directly compensate for the effect of autopilot lag and improve missile intercept performance [13,14]. The integrated design is also less susceptible to actuator saturation and stability problems. Simulations have confirmed the benefits of an IGC design compared to a time-scale separated guidance and control design when applied to the LOS based formation flight problem [12]. However, the previous approach assumed that the ideal values of the LOS variables like range, azimuth and elevation angles and their derivatives were available for feedback in the IGC design.

The contribution of this paper is in developing a method for integrating adaptive estimation and adaptive control designs for a class of uncertain nonlinear systems having both parametric uncertainties and unmodeled dynamics. Lyapunov-like stability analysis is used to prove the UUB of the integrated closed-loop system errors. The presented approach is then applied to a vision-based formation flight control problem. The states of the NN augmented Kalman filter are used to construct estimates of the LOS variables and their derivatives and the outputs of the observer NN are estimates of the leader aircraft acceleration along the inertial axes. The adaptive control solution is based on the adaptive IGC design presented in Ref. [12]. Finally, simulation results using a nonlinear 6DOF simulation model of a fixed-wing UAV are presented. The formation control tracking performance is evaluated using two different leader maneuvers to show the effectiveness of adaptation in the integrated estimation, guidance and control design.

The organization of the paper is as follows. Section II presents the problem formulation for a class of nonlinear systems with parametric uncertainties and unmodeled dynamics. This class of nonlinear systems is an adequate representation of the LOS formation flight problem being considered. Section III contains a discussion of the NN augmented Kalman filter as the adaptive state estimator for the nonlinear system in Section II. Section IV discusses the adaptive control design that is based on approximate feedback linearization and is a function of the estimated states from the adaptive estimator. Section V outlines the Lyapunov-like stability analysis of the closed-loop system with the details of the proof given in the Appendix. Section VI presents the application to the LOS formation flight problem with simulation results. Section VII presents the conclusions of this study.

II. Problem Formulation

Consider the Multi-Input Multi-Output (MIMO) nonlinear system given by

$$
\begin{aligned}
\dot{\boldsymbol{x}}_1 &= A_1\boldsymbol{x}_1 + B_1\left[\boldsymbol{\varsigma}\left(\boldsymbol{x}_2\right) + \boldsymbol{g}\left(\boldsymbol{x}_1, \boldsymbol{z}\right)\right] \\
\boldsymbol{y}_1 &= C_1\boldsymbol{x}_1 \\
\dot{\boldsymbol{z}} &= \boldsymbol{f}_z\left(\boldsymbol{x}_1, \boldsymbol{z}\right) \\
\dot{\boldsymbol{x}}_2 &= \boldsymbol{f}_2\left(\boldsymbol{x}_2\right) + G\left(\boldsymbol{x}_2\right)\boldsymbol{u} \\
\boldsymbol{y} &= \boldsymbol{h}\left(\boldsymbol{y}_1, \boldsymbol{x}_2\right)
\end{aligned}
\tag{1}
$$

where $\boldsymbol{x}_1 \in D_{x_1} \subset \Re^{n_1}$ and $\boldsymbol{x}_2 \in D_{x_2} \subset \Re^{n_2}$ are the modeled states of the system, $\boldsymbol{z} \in D_z \subset \Re^{n_z}$ are the unmodeled states where n_z is also unknown but bounded, D_{x_1}, D_{x_2}, and D_z are open sets containing their respective origins, $\boldsymbol{y}_1 \in \Re^m$ and $\boldsymbol{x}_2$ are measurements available for feedback, and $\boldsymbol{y} \in \Re^p$ and $\boldsymbol{u} \in \Re^p$ are the regulated outputs and control inputs of the system. The matrices $A_1 \in \Re^{n_{x_1} \text{ x } n_{x_1}}$, $B_1 \in \Re^{n_{x_1} \text{ x } m}$ and $C_1 \in \Re^{m \text{ x } n_{x_1}}$ are known, and the pair $\left(A_1, C_1\right)$ is observable. The functions $\boldsymbol{\varsigma} : D_{x_2} \to \Re^m$ and $\boldsymbol{h} : \Re^m \text{ x } D_{x_2} \to \Re^p$ are known and continuous. The functions $\boldsymbol{f}_2 : D_{x_2} \to \Re^{n_2}$ and $G : D_{x_2} \to \Re^{n_2 \text{ x } m}$ are *partially* known and continuous. The function $\boldsymbol{f}_z(\boldsymbol{x}_1, \boldsymbol{z}) : D_{x_1} \times D_z \to \Re^{n_z}$ is unknown, continuous and represents the unmodeled dynamics. The function $\boldsymbol{g}(\boldsymbol{x}_1, \boldsymbol{z}) : D_{x_1} \times D_z \to \Re^m$ is unknown, continuous and represents the way in which the unmodeled dynamics is coupled to the system dynamics. Let $\boldsymbol{x} = \left[\boldsymbol{x}_1^T, \boldsymbol{x}_2^T, \boldsymbol{z}^T\right]^T \in D_{\boldsymbol{x}} \subset \Re^n$, $n = n_{x_1} + n_{x_2} + n_z$, be the composite state vector of the system, where $D_{\boldsymbol{x}} = D_{x_1} \text{ x } D_{x_2} \text{ x } D_z$.

Remark 1: In context of the vision-based formation flight problem, $\boldsymbol{x}_1$ represents the states of the LOS kinematics, $\boldsymbol{x}_2$ represents the states of the rigid body dynamics of the follower aircraft, assumed to be all available, $\boldsymbol{z}$ represents the unknown states associated with the leader acceleration dynamics, $\boldsymbol{y}_1$ represents the measurements obtained via the use of a vision sensor, $\boldsymbol{u}$ represents the actuator deflections of the follower aircraft, and $\boldsymbol{y}$ represents the *measurable* regulated outputs of interest, for example, the measurements from the vision sensor or those obtained by combining outputs from different sensors. The complete state vector $\boldsymbol{x}_1$ is not available for feedback. The unknown functions $\boldsymbol{f}_z(\boldsymbol{x}_1, \boldsymbol{z})$ and $\boldsymbol{g}(\boldsymbol{x}_1, \boldsymbol{z})$ represent the leader acceleration dynamics and the effect of the leader acceleration on the LOS kinematics respectively. The function $\boldsymbol{\varsigma}\left(\boldsymbol{x}_2\right)$ represents the effect of the follower accelerations on the LOS kinematics and hence it is reasonable to assume $\boldsymbol{\varsigma}\left(\boldsymbol{x}_2\right)$ is known. The functions $\boldsymbol{f}_2\left(\boldsymbol{x}_2\right)$ and $G\left(\boldsymbol{x}_2\right)$ represent the follower aircraft dynamics and it is reasonable to assume that at least a linear model of the aircraft dynamics is available implying partial knowledge of $\boldsymbol{f}_2(\cdot)$ and $G(\cdot)$.

Assumption 1: The function $\boldsymbol{f}_z(\cdot,\cdot)$ is a bounded function of its arguments and $\boldsymbol{z}(t)$ is bounded for all t.

Assumption 2: The dynamical system (1) satisfies the conditions for output feedback linearization [4] with vector relative degree $\boldsymbol{r} \triangleq \left[r_1, r_2, \cdots, r_p\right]^T$, $\boldsymbol{r} = r_1 + r_2 + \cdots + r_p \le n$.

Then there exists a mapping $\boldsymbol{\xi} = \boldsymbol{\varphi}\left(\boldsymbol{x}\right) = \boldsymbol{\varphi}\left(\boldsymbol{x}_1, \boldsymbol{x}_2, \boldsymbol{z}\right)$ which is given by

$$
\boldsymbol{\varphi}\left(\boldsymbol{x}\right) = \begin{bmatrix} \boldsymbol{\varphi}_1 \\ \boldsymbol{\varphi}_1 \\ \vdots \\ \boldsymbol{\varphi}_p \end{bmatrix}, \; \boldsymbol{\varphi}_i = \begin{bmatrix} y_i \\ \dot{y}_i \\ \vdots \\ y_i^{(r_i - 1)} \end{bmatrix}
\tag{2}
$$

that transforms the system in (1) into the normal form [4]:

$$
\begin{aligned}
&\dot{\boldsymbol{Z}} = \boldsymbol{f}_{\boldsymbol{Z}}\left(\boldsymbol{\xi}, \boldsymbol{Z}\right) \\
&\dot{\xi}_i^1 = \xi_i^2 \\
&\quad \vdots \\
&\dot{\xi}_i^{(r_i-1)} = \xi_i^{(r_i)} \\
&\dot{\xi}_i^{(r_i)} = \alpha_i^0\left(\boldsymbol{x}_1, \boldsymbol{x}_2\right) + \alpha_i^1\left(\boldsymbol{x}_1, \boldsymbol{x}_2, \boldsymbol{z}, u_i\right) + \beta_i\left(\boldsymbol{y}_1, \boldsymbol{x}_2\right) u_i \\
&y_i = \xi_i^1, \quad i = 1, 2, \cdots, p
\end{aligned}
\tag{3}
$$

where $\boldsymbol{\xi} \triangleq \left[\begin{array}{cccccccccc} \xi_1^1 & \xi_1^2 & \cdots & \xi_1^{(r_i)} & \cdots & \xi_p^1 & \xi_p^2 & \cdots & \xi_p^{(r_p)} \end{array}\right]^T \in D_\xi \subset \Re^r$, $\boldsymbol{Z} \in D_{\boldsymbol{Z}} \subset \Re^{n-r}$ are the states associated with the internal dynamics, u_i are the control inputs, y_i are the regulated outputs, r_i is the relative degree of the i^{th} output, $\boldsymbol{f}_{\boldsymbol{Z}}\left(\boldsymbol{\xi}, \boldsymbol{Z}\right)$ is a completely unknown continuous function representing the internal dynamics, $\alpha_i^0\left(\boldsymbol{x}_1, \boldsymbol{x}_2\right) = \alpha_i^0\left(\boldsymbol{\xi}\right)$ and $\beta_i\left(\boldsymbol{y}_1, \boldsymbol{x}_2\right)$ are known continuous functions, and $\alpha_i^1\left(\boldsymbol{x}_1, \boldsymbol{x}_2, \boldsymbol{z}, u_i\right) = \alpha_i^1\left(\boldsymbol{\xi}, \boldsymbol{Z}, u_i\right)$ are unknown continuous functions.

Assumption 3: The function $\boldsymbol{f}_{\boldsymbol{Z}}\left(\cdot, \cdot\right)$ is a bounded function of its arguments and $\boldsymbol{Z}\left(t\right)$ is bounded for all t.

Assumption 4: $\beta_i\left(\boldsymbol{y}_1, \boldsymbol{x}_2\right)$ is continuous and non-zero for every $\boldsymbol{x} \in D_{\boldsymbol{x}}$.

Control Design Objective: Design a control law as a function of available measurements such that $y_i\left(t\right)$ track smooth, bounded reference trajectories $y_{c,i}\left(t\right)$, $i = 1, 2, \cdots, p$ with bounded errors.

In the case when the states $\boldsymbol{x}_1$ are available for feedback, an approach to controller design for achieving the above objective is to consider a feedback linearizing solution augmented with the output of adaptive NNs designed to approximate the unknown functions $\alpha_i^1\left(\boldsymbol{x}_1, \boldsymbol{x}_2, \boldsymbol{z}, u_i\right)$. When the states $\boldsymbol{x}_1$ are not available, we design a state estimator to provide estimates of $\boldsymbol{x}_1$ for implementation in the adaptive control solution. These estimates are also used to construct estimates of the functions $\alpha_i^0\left(\boldsymbol{x}_1, \boldsymbol{x}_2\right)$ in the control solution.

III. Adaptive State Estimation

The objective of the adaptive estimation is to provide estimates of the states $\boldsymbol{x}_1$. The estimator solution must be robust to the effect of the unmodeled dynamics. The adaptive state estimation solution considered in this paper is a time-varying Kalman filter augmented with an adaptive NN that is updated online using only the available measurements. In particular, we employ a modified method of composite adaptation, i.e., using two training signals to train the same NN, to improve the ability of the NN to approximate the unmodeled dynamics [2].

We consider only the following subsystem for the state estimation problem

$$
\begin{aligned}
&\dot{\boldsymbol{x}}_1 = A_1 \boldsymbol{x}_1 + B_1\left[\varsigma\left(\boldsymbol{x}_2\right) + \boldsymbol{g}\left(\boldsymbol{x}_1, \boldsymbol{z}\right)\right], \quad \boldsymbol{x}_1(t_0) = \boldsymbol{x}_{10} \\
&\boldsymbol{y}_1 = C_1 \boldsymbol{x}_1 \\
&\dot{\boldsymbol{z}} = \boldsymbol{f}_z\left(\boldsymbol{x}_1, \boldsymbol{z}\right), \quad \boldsymbol{z}(t_0) = \boldsymbol{z}_0
\end{aligned}
\tag{4}
$$

The theorem presented next is critical to the use of a NN as the adaptive element in the state estimation problem.

Theorem 1 [22]: Assume that a n dimensional state vector $\boldsymbol{x}(t)$ of an observable time-invariant system

$$\begin{aligned} \dot{\boldsymbol{x}} &= \boldsymbol{f}(\boldsymbol{x}) \\ \boldsymbol{y} &= \boldsymbol{h}(\boldsymbol{x}) \end{aligned} \tag{5}$$

evolves on a n dimensional ball of radius $\bar{r}$ in R^n, $B_{\bar{r}} = \left\{ \boldsymbol{x} \in R^n \mid \|\boldsymbol{x}\| < \bar{r} \right\}$. Also assume that the system output $\boldsymbol{y}(t) \in R^m$ and its derivatives up to the order $(n-1)$ are bounded. Then given arbitrary $\varepsilon^* > 0$, there exists a set of constant, bounded weights W and a positive time delay $d > 0$, such that the function $\boldsymbol{f}(\boldsymbol{x})$ in (5) can be approximated over the compact set $B_{\bar{r}}$ by a linearly parameterized NN

$$\boldsymbol{f}(\boldsymbol{x}) = W^T \boldsymbol{\sigma}(\bar{\boldsymbol{\mu}}) + \boldsymbol{\varepsilon}(\bar{\boldsymbol{\mu}}), \ \|W\|_F \le W^*, \ \|\boldsymbol{\varepsilon}(\bar{\boldsymbol{\mu}})\| \le \varepsilon^*, \ \|\bar{\boldsymbol{\mu}}\| \le \mu^* \tag{6}$$

using the input vector

$$\bar{\boldsymbol{\mu}}(\boldsymbol{y}(t), d) = \left[\Delta_d^{(0)} \boldsymbol{y}^T(t) \ \ \ldots \ \ \Delta_d^{(n-1)} \boldsymbol{y}^T(t) \right] \ \in R^{nm} \tag{7}$$

where $\Delta_d^{(0)} \boldsymbol{y}^T(t) = \boldsymbol{y}^T(t)$, $\Delta_d^{(k)} \boldsymbol{y}^T(t) = \dfrac{\Delta_d^{(k-1)} \boldsymbol{y}^T(t) - \Delta_d^{(k-1)} \boldsymbol{y}^T(t-d)}{d}$, $k = 1, 2, \ldots,$, $\mu^* > 0$ is a uniform bound on $B_{\bar{r}}$.

The above theorem simply states the conditions under which the unknown function $\boldsymbol{f}(\boldsymbol{x})$ can be approximated by a NN on a compact domain using a finite sample of the time history of the measurements given by the input vector $\bar{\boldsymbol{\mu}}(\boldsymbol{y}(t), d)$.

We assume that $B_1 \boldsymbol{g}(\boldsymbol{x}_1, \boldsymbol{z})$ can be written in the form

$$B_1 \boldsymbol{g}(\boldsymbol{x}_1, \boldsymbol{z}) = \sum_{i=1}^{m} \boldsymbol{b}_i g_i'(\boldsymbol{x}_1, \boldsymbol{z}) \tag{8}$$

where $\boldsymbol{b}_i$ is a column vector of zeros with only the i^{th} element equal to 1.Using Theorem 1, consider the following NN parameterization of the unmodeled dynamics $g_i'(\boldsymbol{x}_1, \boldsymbol{z})$

$$\begin{aligned} g_i'(\boldsymbol{x}_1, \boldsymbol{z}) &= \boldsymbol{W}_{o,i}{}^T \boldsymbol{\sigma}_o(\bar{\boldsymbol{\mu}}_o) + \varepsilon_{o,i}'(\bar{\boldsymbol{\mu}}_o), \ \ \|\boldsymbol{W}_{o,i}\|_F \le W_{o,i}^* \le W_o^*, \ \ \|\varepsilon_{o,i}'(\bar{\boldsymbol{\mu}})\| \le \varepsilon_{o,i}^* \le \varepsilon_o^*, \\ \bar{\boldsymbol{\mu}}_o &\in B_{\mu_o^*} = \left\{ \bar{\boldsymbol{\mu}}_o \ \mid \ \|\bar{\boldsymbol{\mu}}_o\| \le \mu_o^* \right\}, \ \ i = 1, 2, \cdots, m \end{aligned} \tag{9}$$

$\forall (\boldsymbol{x}_1, \boldsymbol{x}_2, \boldsymbol{z}) \in D_g \subset D_{x_1} \text{ x } D_{x_2} \text{ x } D_z$, where D_g is a compact set, the subscript 'o' stands for 'observer', $\boldsymbol{W}_{o,i} \in \Re^{N_o}$ is the ideal but unknown NN weight vector, $\varepsilon_{o,i}(\bar{\boldsymbol{\mu}}_o)$ is the NN functional approximation error, $\boldsymbol{\sigma}_o(\bar{\boldsymbol{\mu}}_o) = \left[\sigma_{o,1}(\bar{\boldsymbol{\mu}}_o), \ldots, \sigma_{o,N_o}(\bar{\boldsymbol{\mu}}_o) \right]^T$ is a vector of sigmoidal functions $\sigma_{o,i}(\cdot)$, N_o is the number of neurons, W_o^* and ε_o^* are the bounds on the Frobenius norms of $\boldsymbol{W}_{o,i}$ and $\varepsilon_{o,i}$ respectively, and the input vector $\bar{\boldsymbol{\mu}}_o = \bar{\boldsymbol{\mu}}_o(\boldsymbol{y}_1(t), \boldsymbol{\varsigma}(t-d), d)$ is a vector of difference quotients of the output vector $\boldsymbol{y}_1$ and known vector $\boldsymbol{\varsigma}$,

$$\begin{aligned}
&\bar{\boldsymbol{\mu}}_o\left(\boldsymbol{y}_1(t),\boldsymbol{\varsigma}(t-d),d\right)=\left[1,\bar{\boldsymbol{y}}_{1,d}^T(t),\ \bar{\boldsymbol{\varsigma}}_d^T(t-d)\right]^T\\
&\bar{\boldsymbol{y}}_{1,d}^T(t)=\left[\Delta_d^{(0)}\boldsymbol{y}_1^T(t),\ \cdots,\Delta_d^{(n_1-1)}\boldsymbol{y}_1^T(t)\right]^T\\
&\bar{\boldsymbol{\varsigma}}_d^T(t-d)=\left[\Delta_d^{(0)}\boldsymbol{\varsigma}^T(t-d),\ \ldots\ \Delta_d^{(n_2-1)}\boldsymbol{\varsigma}^T(t-d)\right]^T
\end{aligned}\tag{10}$$

where the definitions of the difference quotients $\Delta_d^{(k)}[\cdot]$, $k=1,2,\cdots$ are as in (7), $n_1,n_2\geq n$ are sufficiently large integers, and $d>0$ is the time delay. The sigmoidal functions are smooth and uniformly bounded, that is, $\left|\sigma_{o,i}\left(\bar{\boldsymbol{\mu}}_o\right)\right|\leq 1$. Using Eqs. (8) and (9), the system equation in (4) can be written as:

$$\begin{aligned}
&\dot{\boldsymbol{x}}_1=A_1\boldsymbol{x}_1+B_1\boldsymbol{\varsigma}+\sum_i^m\boldsymbol{b}_i\boldsymbol{W}_{o,i}{}^T\boldsymbol{\sigma}_o\left(\bar{\boldsymbol{\mu}}_o\right)+\sum_i^m\boldsymbol{b}_i\varepsilon_{o,i}^{'}\left(\bar{\boldsymbol{\mu}}_o\right)\\
&\dot{\boldsymbol{z}}=\boldsymbol{f}_z\left(\boldsymbol{x}_1,\boldsymbol{z}\right),\\
&\boldsymbol{y}_1=C_1\boldsymbol{x}_1
\end{aligned}\tag{11}$$

The adaptive estimator for the system in (11) is given by

$$\begin{aligned}
&\dot{\hat{\boldsymbol{x}}}_1(t)=A_1\hat{\boldsymbol{x}}_1(t)+K_1(t)\left(\boldsymbol{y}_1(t)-\hat{\boldsymbol{y}}_1(t)\right)+B_1\boldsymbol{\varsigma}+\sum_i^m\boldsymbol{b}_i\hat{\boldsymbol{W}}_{o,i}{}^T(t)\boldsymbol{\sigma}_o\left(\bar{\boldsymbol{\mu}}_o\right),\qquad \hat{\boldsymbol{x}}_1(t_0)=\hat{\boldsymbol{x}}_{10}\\
&\hat{\boldsymbol{y}}_1(t)=C_1\hat{\boldsymbol{x}}_1(t)
\end{aligned}\tag{12}$$

where $\hat{\boldsymbol{W}}_{o,i}\ (t)$ is an estimate of the ideal but unknown NN weight vector $\boldsymbol{W}_{o,i}$, $K_1(t)$ is the Kalman gain obtained through the following set of matrix differential Ricatti equations [21]

$$\begin{aligned}
&\dot{P}_1(t)=A_1P_1(t)+P_1(t)A_1^T-P_1(t)C_1^TR_1^{-1}C_1P_1(t)+Q_1\\
&K_1(t)=P_1(t)C_1^TR_1^{-1}
\end{aligned}\tag{13}$$

where $P_1(0)=P_0>0,\ Q_1=Q_1^T>0,\ R_1=R_1^T>0$. The solution $P_1(t)$ of Eq. (13) is bounded, symmetric, positive definite and continuously differentiable. The output of the i^{th} observer NN is given by

$$\hat{g}_i\left(t\right)=\hat{\boldsymbol{W}}_{o,i}\left(t\right)^T\boldsymbol{\sigma}_o\left(\bar{\boldsymbol{\mu}}_o\right),\ i=1,2,\cdots,m\tag{14}$$

The residual vector of the adaptive estimator $\tilde{\boldsymbol{y}}_1\left(t\right)=\boldsymbol{y}_1\left(t\right)-\hat{\boldsymbol{y}}_1\left(t\right)$ is the first set of error signals used to train the NN as in Ref. [8].

Now consider a second, non-adaptive Kalman filter whose residuals are used to construct the second error signal used to train the NN

$$\begin{aligned}
&\dot{\hat{\boldsymbol{x}}}_{na,1}(t)=A_1\hat{\boldsymbol{x}}_{na,1}(t)+K_{na,1}(t)\left(\boldsymbol{y}_1(t)-\hat{\boldsymbol{y}}_{na,1}(t)\right)+B_1\boldsymbol{\varsigma},\qquad \hat{\boldsymbol{x}}_{na1}(t_0)=\hat{\boldsymbol{x}}_{na,10}\\
&\hat{\boldsymbol{y}}_{na,1}(t)=C_1\hat{\boldsymbol{x}}_{na,1}(t)
\end{aligned}\tag{15}$$

where the subscript '*na*' is used to identify this second filter as a non-adaptive filter and $K_{na,1}(t)$ is the Kalman gain obtained through the following set of matrix differential Ricatti equations [21]

$$\begin{aligned}
&\dot{P}_{na,1}(t)=A_1P_{na,1}(t)+P_{na,1}(t)A_1^T-P_{na,1}(t)C_1^TR_{na,1}^{-1}C_1P_{na,1}(t)+Q_{na,1}\\
&K_{na,1}(t)=P_{na,1}(t)C_1^TR_{na,1}^{-1}
\end{aligned}\tag{16}$$

where $P_{na,1}(0) = P_{na,10} = P_0 > 0$, $Q_{na,1} = Q_{na,1}{}^T > 0$, $R_{na,1} = R_{na,1}^T > 0$. The solution $P_{na,1}(t)$ of eq. (16) is bounded, symmetric, positive definite and continuously differentiable. The design matrices $Q_{na,1}$ and $R_{na,1}$ can be chosen to be different from Q_1 and R_1 respectively in eq. (13).

The state estimation error dynamics of the second Kalman filter is obtained from Eqs. (11) and (15) by defining $\tilde{\boldsymbol{x}}_{na,1} \triangleq \boldsymbol{x}_1 - \hat{\boldsymbol{x}}_{na,1}$ as the state estimation error vector:

$$\begin{aligned} \dot{\tilde{\boldsymbol{x}}}_{na,1} &= \bar{A}_{na,1}(t)\tilde{\boldsymbol{x}}_{na,1} + \sum_i^m \boldsymbol{b}_i \boldsymbol{W}_{o,i}{}^T \boldsymbol{\sigma}_o(\bar{\boldsymbol{\mu}}_o) + \sum_i^m \boldsymbol{b}_i \varepsilon_{o,i}'(\bar{\boldsymbol{\mu}}_o) \\ \tilde{\boldsymbol{y}}_{na,1} &= C_1 \tilde{\boldsymbol{x}}_{na,1} \end{aligned} \tag{17}$$

where $\tilde{\boldsymbol{y}}_{na,1} \triangleq \boldsymbol{y}_1 - \hat{\boldsymbol{y}}_{na,1}$ is the residual and $\bar{A}_{na,1}(t) = A_1 - K_{na,1}(t)C_1$. The time-domain solution of the residual vector in (17) is given by

$$\tilde{\boldsymbol{y}}_{na,1}(t) = C_1 \Phi_{na,1}(t,t_0)\tilde{\boldsymbol{x}}_{na,1}(t_0) + \sum_i^m \int_{t_0}^t C_1 \Phi_{na,1}(t,\tau)\boldsymbol{b}_i \boldsymbol{W}_{o,i}{}^T \boldsymbol{\sigma}_o(\bar{\boldsymbol{\mu}}_o)\ d\tau + \sum_i^m \int_{t_0}^t C_1 \Phi_{na,1}(t,\tau)\boldsymbol{b}_i \varepsilon_{o,i}'\ d\tau \tag{18}$$

where $\Phi_{na,1}(t,t_0)$ is the state transition matrix associated with the matrix $\bar{A}_{na,1}(t)$. We now state and prove a key Lemma.

Lemma 1: The estimation error dynamics of the unforced system

$$\begin{aligned} \dot{\tilde{\boldsymbol{x}}}_{na,1} &= \bar{A}_{na,1}(t)\tilde{\boldsymbol{x}}_{na,1} \\ \tilde{\boldsymbol{y}}_{na,1} &= C_1 \tilde{\boldsymbol{x}}_{na,1} \end{aligned} \tag{19}$$

are Globally Exponentially Stable (GES). This implies that

$$\Phi_{na,1}(t,t_0)\tilde{\boldsymbol{x}}_{na,1}(t_0) \to 0, \ \text{ as } \ t \to \infty, \ \ \forall t \geq t_0 \geq 0 \tag{20}$$

where $\Phi_{na,1}(t,t_0)$ is the state transition matrix of the system (19). The above result implies that in presence of bounded input $\boldsymbol{g}(\boldsymbol{x}_1, z)$ to the system in (19), the estimation error vector $\tilde{\boldsymbol{x}}_{na,1}(t)$ and the residual $\tilde{\boldsymbol{y}}_{na,1}(t)$ are bounded.

Proof: In the Appendix.

Remark 2: The NN approximation of the unmodeled dynamics in (9) and the boundedness of $\tilde{\boldsymbol{x}}_{na,1}(t)$ are contingent on $g_i'(\boldsymbol{x}_1, \boldsymbol{z})$, $i = 1,2,\cdots,m,$ being bounded. The states $\boldsymbol{z}$ are bounded as a result of Assumption 1. Since $g_i'(\boldsymbol{x}_1, \boldsymbol{z})$ is continuous, to show that $g_i'(\boldsymbol{x}_1, \boldsymbol{z})$ is bounded, we need to show that the states evolve in a compact set. Since the boundedness of the states is not assured *a priori* in a combined estimation and control problem, one way to ensure the states evolve in a compact set is to make an assumption that the initial state estimation errors belong to a Lyapunov level set such that the input variables to the NNs lie within the compact set D_g defined in (9). This is stated below *Remark 4*. The proof of boundedness will then show that the errors ultimately go to a Lyapunov level set that lies completely within the Lyapunov level set that contains the initial errors.

Now, we continue on with the derivation of the second error signal to train the NN. Taking advantage of the fact that $\boldsymbol{W}_{o,i}$ is a vector, eq. (18) can be re-written as

$$\tilde{\boldsymbol{y}}_{na,1}(t) = T_1\left(\tilde{\boldsymbol{x}}_{na,1}(t_0), \varepsilon_{f1}^{'}, \varepsilon_{f2}^{'}, \cdots, \varepsilon_{fm}^{'}\right) + \sum_i^m \int_{t_0}^{t} \underbrace{\left[C_1 \Phi_{na,1}(t,\tau)\boldsymbol{b}_i \boldsymbol{\sigma}_o^T\left(\bar{\boldsymbol{\mu}}_o\right) d\tau\right]}_{Q_{fi}} \boldsymbol{W}_{o,i} \tag{21}$$

where $T_1\left(\tilde{\boldsymbol{x}}_{na,1}(t_0), \varepsilon_{f1}^{'}, \varepsilon_{f2}^{'}, \cdots, \varepsilon_{fm}^{'}\right) = C_1 \Phi_{na,1}(t,t_0)\tilde{\boldsymbol{x}}_{na,1}(t_0) + \sum_i^m \int_{t_0}^{t} C_1 \Phi_{na,1}(t,\tau)\boldsymbol{b}_i \varepsilon_{o,i}^{'} \; d\tau$ is an unknown vector that is always bounded using the result of Lemma 1, and Q_{fi} is the filtered basis function matrix obtained by solving the following matrix differential equation:

$$\begin{aligned} \dot{\Omega}_{fi} &= \bar{A}_{na,1}(t)\Omega_{fi} + \boldsymbol{b}_i \boldsymbol{\sigma}_o^T\left(\bar{\boldsymbol{\mu}}_o\right), \;\; \Omega_{fi}(t_0) = 0 \\ Q_{fi} &= C_1 \Omega_{fi} \end{aligned} \tag{22}$$

The matrix $\Omega_{fi} \in \Re^{n_1 \text{ x } N_o}$ is always bounded, again using the result of Lemma 1 and the output matrix $Q_{fi} \in \Re^{m \text{ x } N_o}$ is similarly bounded. An estimate of $\tilde{\boldsymbol{y}}_{na,1}(t)$ is obtained by using $\hat{\boldsymbol{W}}_{o,i}(t)$ in place of $\boldsymbol{W}_{o,i}$ in (21)

$$\hat{\tilde{\boldsymbol{y}}}_{na,1}(t) = \sum_i^m Q_{fi} \hat{\boldsymbol{W}}_{o,i} \tag{23}$$

The signal formed by the difference between $\tilde{\boldsymbol{y}}_{na,1}(t)$ and its estimate $\hat{\tilde{\boldsymbol{y}}}_{na,1}(t)$ is the second error signal used to train the NN

$$\boldsymbol{e}_{na,1}(t) = \tilde{\boldsymbol{y}}_{na,1}(t) - \hat{\tilde{\boldsymbol{y}}}_{na,1}(t) = \tilde{\boldsymbol{y}}_{na,1}(t) - \sum_i^m Q_{fi} \hat{\boldsymbol{W}}_{o,i} \tag{24}$$

and the NN composite adaptive law is given by

$$\dot{\hat{\boldsymbol{W}}}_{o,i} = -\Gamma_{o,i}\left\{-\boldsymbol{\sigma}_o\left(\bar{\boldsymbol{\mu}}_o\right)\tilde{y}_{1,i} - Q_{fi}^T \boldsymbol{e}_{na,1} + \lambda_o \hat{\boldsymbol{W}}_{o,i}\right\} \tag{25}$$

where $\tilde{y}_{1,i}$ is the i^{th} element of the residual vector $\tilde{\boldsymbol{y}}_1$, and the adaptation gain $\Gamma_{o,i} > 0$ and the robustifying sigma-mod term [23] $\lambda_o > 0$ are NN design constants.

IV. Adaptive Control Design

We demonstrate the adaptive control design for only the i^{th} regulated output and start with the normal form given in Eq. (3):

$$\begin{aligned} y_i &= h_i\left(\boldsymbol{y}_1, \boldsymbol{x}_2\right) \\ y_i^{(r_i)} &= \alpha_i^0\left(\boldsymbol{x}_1, \boldsymbol{x}_2\right) + \alpha_i^1\left(\boldsymbol{x}_1, \boldsymbol{x}_2, \boldsymbol{z}, u_i\right) + \beta_i\left(\boldsymbol{y}_1, \boldsymbol{x}_2\right)u_i \end{aligned} \tag{26}$$

where r_i is the relative degree of y_i and is assumed to be known. Eq. (26) can be re-written as follows:

$$y_i^{(r_i)} = \alpha_i^0\left(\hat{\boldsymbol{x}}_1, \boldsymbol{x}_2\right) + \beta_i\left(\hat{\boldsymbol{y}}_1, \boldsymbol{x}_2\right)u_i + \Delta_{c,i}\left(\boldsymbol{x}_1, \hat{\boldsymbol{x}}_1, \boldsymbol{x}_2, \boldsymbol{z}, u_i\right) \tag{27}$$

where

$$\Delta_{c,i}\left(\boldsymbol{x}_1, \hat{\boldsymbol{x}}_1, \boldsymbol{x}_2, \boldsymbol{z}, u_i\right) = \left[\alpha_i^0\left(\boldsymbol{x}_1, \boldsymbol{x}_2\right) - \alpha_i^0\left(\hat{\boldsymbol{x}}_1, \boldsymbol{x}_2\right)\right] + \left[\beta_i\left(\boldsymbol{y}_1, \boldsymbol{x}_2\right) - \beta_i\left(\hat{\boldsymbol{y}}_1, \boldsymbol{x}_2\right)\right]u_i + \alpha_i^1\left(\boldsymbol{x}_1, \boldsymbol{x}_2, \boldsymbol{z}, u_i\right) \tag{28}$$

A. Tracking Error Dynamics and Feedback Inversion Control Law

The control design objective is to design a control law as a function of available measurements such that $y_i(t)$ tracks smooth, bounded reference trajectories $y_{c,i}(t)$, $i = 1, 2, \cdots, p$ with bounded errors. The tracking error is defined as $e_i = y_{c,i} - y_i$, where the reference signal $y_{c,i}$ and its derivatives $\dot{y}_{c,i}, \ddot{y}_{c,i}, \cdots, y_{c,i}^{(r_i)}$ are generated by filtering a piece-wise continuous, bounded command $y_{com,i}(t)$ through asymptotically stable reference models. The r_i^{th} derivative of e_i is given by:

$$e_i^{(r_i)} = y_{c,i}^{(r_i)} - y_i^{(r_i)} = y_{c,i}^{(r_i)} - \alpha_i^0\left(\hat{\boldsymbol{x}}_1, \boldsymbol{x}_2\right) - \beta_i\left(\hat{\boldsymbol{y}}_1, \boldsymbol{x}_2\right)u_i - \Delta_{c,i}\left(\boldsymbol{x}_1, \hat{\boldsymbol{x}}_1, \boldsymbol{x}_2, \boldsymbol{z}, u_i\right) \tag{29}$$

Assumption 5: $\beta_i\left(\hat{\boldsymbol{y}}_1, \boldsymbol{x}_2\right)$ is non-zero for every $\left(\boldsymbol{x}, \hat{\boldsymbol{x}}_1\right) \in D_{\boldsymbol{x}}$ x $D_{\boldsymbol{x}_1}$, where $\hat{\boldsymbol{x}}_1$ evolves in the open set $D_{\boldsymbol{x}_1} \subset \Re^{n_{x1}}$ that contains the origin $\hat{\boldsymbol{x}}_1 = \boldsymbol{0}$.

A feedback inversion control law for stabilizing the error dynamics in (29) is given by

$$u_i = \frac{\nu_i}{\beta_i\left(\hat{\boldsymbol{y}}_1, \boldsymbol{x}_2\right)} \tag{30}$$

where ν_i is the pseudo-control term given by

$$\nu_i = y_{c,i}^{(r_i)} - \alpha_i^0\left(\hat{\boldsymbol{x}}_1, \boldsymbol{x}_2\right) + \nu_{dc,i} - \nu_{ad,i} \tag{31}$$

Substituting Eqs. (30)and (31) into (29), we have

$$e_i^{(r_i)} = -\nu_{dc,i} + \nu_{ad,i} - \Delta_{c,i}\left(\boldsymbol{x}_1, \hat{\boldsymbol{x}}_1, \boldsymbol{x}_2, \boldsymbol{z}, \nu_i\right) \tag{32}$$

where $\nu_{dc,i}$ is the output of a linear compensator designed to stabilize the linearized error dynamics

$$e_i^{(r_i)} = -\nu_{dc,i} \tag{33}$$

and $\nu_{ad,i}$ is the output of an adaptive NN designed to compensate for the modeling error function $\Delta_{c,i}\left(\boldsymbol{x}_1, \hat{\boldsymbol{x}}_1, \boldsymbol{x}_2, \boldsymbol{z}, \nu_i\right)$. Notice that we changed the last argument in $\Delta_{c,i}$ from u_i to ν_i using Eq. (30).

We follow the approach in Ref. 20 for the design of $\nu_{dc,i}$ and $\nu_{ad,i}$. Defining $\boldsymbol{e}_i = \left[e_i, \dot{e}_i, \cdots, e_i^{(r_i-1)}\right]^T$, we have:

$$\begin{aligned} \dot{\boldsymbol{e}}_i &= A_{E,i}\boldsymbol{e}_i + B_{E,i}\left(\nu_{ad,i} - \Delta_{c,i}\right) \\ e_i &= C_{E,i}\boldsymbol{e}_i \end{aligned} \tag{34}$$

where $A_{E,i} = \begin{bmatrix} 0 & 1 & 0 & \cdots & 0 \\ 0 & 0 & 1 & \cdots & 0 \\ \vdots & & \vdots & & \vdots \\ 0 & 0 & 0 & \cdots & 0 \end{bmatrix}_{r_i \text{ x } r_i}$, $B_{E,i} = \begin{bmatrix} 0 \\ 0 \\ \vdots \\ 1 \end{bmatrix}_{r_i \text{ x } 1}$, $C_{E,i} = \begin{bmatrix} 1 & 0 & \cdots & 0 \end{bmatrix}_{1 \text{ x } r_i}$.

Since $\dot{e}_i, \cdots, e_i^{(r_i-1)}$ are not measurable, we design the following lead compensator to stabilize the error dynamics in (34):

$$\begin{aligned} \dot{\boldsymbol{\eta}}_i &= A_{c,i}\boldsymbol{\eta}_i + \boldsymbol{b}_{c,i}e_i \\ \nu_{dc,i} &= \boldsymbol{c}_{c,i}\boldsymbol{\eta}_i + d_{c,i}e_i \end{aligned} \tag{35}$$

where $\boldsymbol{\eta}_i$ has dimension $\geq r_i - 1$. We assume the minimum dimension for $\boldsymbol{\eta}_i$. Defining $\boldsymbol{E}_i = \left[\boldsymbol{e}_i^T,\ \boldsymbol{\eta}_i^T\right]^T$, we can combine the error dynamics in (34) and the linear compensator dynamics in (35) to give:

$$\begin{aligned} \dot{\boldsymbol{E}}_i &= \bar{A}_{E,i}\boldsymbol{E}_i + \bar{B}_{E,i}\left(\nu_{ad,i} - \Delta_{c,i}\right) \\ \boldsymbol{z}_{E,i} &= \bar{C}_{E,i}\boldsymbol{E}_i = \left[e_i,\ \boldsymbol{\eta}_i^T\right]^T \end{aligned} \tag{36}$$

The lead compensator parameters $\left(A_{c,i}, \boldsymbol{b}_{c,i}, \boldsymbol{c}_{c,i}, d_{c,i}\right)$ are designed such that the matrix $\bar{A}_{E,i}$ is Hurwitz. The $\boldsymbol{E}_i$ dynamics in (36) are henceforth referred to as tracking error dynamics. Since $\bar{A}_{E,i}$ is Hurwitz, then for any $Q_{E,i} > 0$, there exists a unique solution $P_{E,i} = P_{E,i}^T > 0$ of the following Lyapunov equation:

$$\bar{A}_{E,i}^T P_{E,i} + P_{E,i}\bar{A}_{E,i} = -Q_{E,i}, \quad Q_{E,i} = Q_{E,i}^T > 0 \tag{37}$$

B. Error Observer and Neural Network Adaptive Law

Since the complete error vector is not available in the output feedback case, we design a linear *error* observer [25] for the tracking error dynamics in (36). The states of the error observer are estimates of $\boldsymbol{E}_i$ and are used in the construction of the adaptive law. The error observer is given by:

$$\begin{aligned} \dot{\hat{\boldsymbol{E}}}_i &= \bar{A}_{E,i}\hat{\boldsymbol{E}}_i + \bar{K}_{E,i}\left(\boldsymbol{z}_{E,i} - \hat{\boldsymbol{z}}_{E,i}\right) \\ \hat{\boldsymbol{z}}_{E,i} &= \bar{C}_{E,i}\hat{\boldsymbol{E}}_i \end{aligned} \tag{38}$$

where $\bar{K}_{E,i} \neq \left[\boldsymbol{0}\right]$ is the error observer gain matrix that places the poles of the matrix $\tilde{A}_{E,i} = \bar{A}_{E,i} - \bar{K}_{E,i}\bar{C}_{E,i}$ much further to the left of the poles of the error dynamics matrix $\bar{A}_{E,i}$.

Remark 3: The NN adaptive law can be derived without constructing an error observer by applying the direct approach in Ref. 25. The training signal for the NN in this case is obtained by filtering the tracking error through a strictly positive real (SPR) filter.

Defining $\tilde{\boldsymbol{E}}_i = \boldsymbol{E}_i - \hat{\boldsymbol{E}}_i$, the error dynamics of the error observer is given by:

$$\begin{aligned} \dot{\tilde{\boldsymbol{E}}}_i &= \tilde{A}_{E,i}\tilde{\boldsymbol{E}}_i + \bar{B}_{E,i}\left(\nu_{ad,i} - \Delta_{c,i}\right) \\ \tilde{\boldsymbol{z}}_{E,i} &= \bar{C}_{E,i}\tilde{\boldsymbol{E}}_i \end{aligned} \tag{39}$$

Consider the parameterization of the modeling error function $\Delta_{c,i}$ with a linear-in-parameters NN:

$$\Delta_{c,i}\left(\boldsymbol{x}_1,\hat{\boldsymbol{x}}_1,\boldsymbol{x}_2,z,\nu_i\right)=\boldsymbol{W}_{c,i}^T\boldsymbol{\sigma}_c\left(\bar{\boldsymbol{\mu}}_c\right)+\varepsilon_{c,i}\left(\bar{\boldsymbol{\mu}}_c\right),\ \left\|\boldsymbol{W}_{c,i}\right\|_F\le W_{c,i}^*\le W_c^*,\ \left\|\varepsilon_{c,i}\left(\bar{\boldsymbol{\mu}}_c\right)\right\|\le\varepsilon_{c,i}^*\le\varepsilon_c^*,$$
$$\bar{\boldsymbol{\mu}}_c\in B_{\mu_c^*}=\left\{\bar{\boldsymbol{\mu}}_c\ \middle|\ \left\|\bar{\boldsymbol{\mu}}_c\right\|\le\mu_c^*\right\},\ \ i=1,2,\cdots,m \tag{40}$$

$\forall\left(\boldsymbol{x}_1,\boldsymbol{x}_2,\boldsymbol{z},\hat{\boldsymbol{x}}_1,\nu_i\right)\in D_{g_1}\subset D_{x_1}\text{ x }D_{x_2}\text{ x }D_z\text{ x }D_{\dot{x}_1}\text{ x }D_{\boldsymbol{u}}$, where $D_{\boldsymbol{u}}\subset\Re$ and D_{g_1} is a compact set, the subscript '*c*' stands for 'controller', $\boldsymbol{W}_{c,i}\in\Re^{N_c}$ is the ideal but unknown NN weight vector, $\varepsilon_{c,i}\left(\bar{\boldsymbol{\mu}}_c\right)$ is the NN functional approximation error, $\bar{\boldsymbol{\mu}}_c$ is the input vector, $\boldsymbol{\sigma}_c\left(\bar{\boldsymbol{\mu}}_c\right)=\left[\sigma_{c,1}\left(\bar{\boldsymbol{\mu}}_c\right),\ldots,\sigma_{c,N_c}\left(\bar{\boldsymbol{\mu}}_c\right)\right]^T$ is a vector of smooth and uniformly bounded *shifted* sigmoidal functions $\sigma_{c,i}\left(\cdot\right)$ [26, 27], N_c is the number of neurons, and W_c^* and ε_c^* are the bounds on the Frobenius norms of $\boldsymbol{W}_{c,i}$ and $\varepsilon_{c,i}$ respectively. The input vector $\bar{\boldsymbol{\mu}}_c=\bar{\boldsymbol{\mu}}_c\left(\bar{\boldsymbol{\mu}}_o\left(t\right),\hat{\boldsymbol{x}}_1\left(t\right),\boldsymbol{x}_2\left(t\right),\nu_i\left(t-d\right),d\right)$ consists of the input vector to the observer NN $\bar{\boldsymbol{\mu}}_o\left(t\right)$ given in Eq. (10), the estimates of the states $\hat{\boldsymbol{x}}_1$ which are the outputs of the adaptive state estimator described in the previous section, the available states $\boldsymbol{x}_2$, and the delayed values of the pseudo-control signal ν_i:

$$\begin{aligned}\bar{\boldsymbol{\mu}}_c\left(\bar{\boldsymbol{\mu}}_o\left(t\right),\hat{\boldsymbol{x}}_1\left(t\right),\boldsymbol{x}_2\left(t\right),\nu_i\left(t-d\right),d\right)&=\left[1,\bar{\boldsymbol{\mu}}_o^T\left(t\right),\ \hat{\boldsymbol{x}}_1^T\left(t\right),\boldsymbol{x}_2^T\left(t\right),\bar{\boldsymbol{\nu}}_{i,d}^T\left(t-d\right)\right]^T\\ \bar{\boldsymbol{\nu}}_{i,d}\left(t-d\right)&=\left[\Delta_d^{(0)}\nu_i\left(t-d\right),\ \ldots\ \Delta_d^{(n_3-1)}\nu_i\left(t-d\right)\right]^T\end{aligned} \tag{41}$$

where $n_3\ge n$ is a sufficiently large integer, and $d>0$ is the time delay.

From Eqs. (40) and (31), $\Delta_{c,i}$ is a function of $\nu_{ad,i}$ and $\nu_{ad,i}$ is to be designed to cancel $\Delta_{c,i}$. Therefore the following assumption is introduced to guarantee existence and uniqueness of a solution for $\nu_{ad,i}$.

Assumption 6: The mapping $\nu_{ad_i}\mapsto\Delta_{c,i}$ is a contraction over the entire input domain of interest [24, 25].

Assumption 6 is satisfied if the following two conditions are satisfied [25]:

$$\begin{aligned}&\text{i) }\operatorname{sign}\left(\frac{\partial y_i^{(r_i)}}{\partial u_i}\right)=\operatorname{sign}\left(\frac{\partial\nu_i}{\partial u_i}\right)\Rightarrow\operatorname{sign}\left(\frac{\partial\alpha_i^1}{\partial u_i}+\beta_i\left(\boldsymbol{y}_1,\boldsymbol{x}_2\right)\right)=\operatorname{sign}\left(\beta_i\left(\hat{\boldsymbol{y}}_1,\boldsymbol{x}_2\right)\right)\\&\text{ii)}\left|\frac{\partial\nu_i}{\partial u_i}\right|>\frac{1}{2}\left|\frac{\partial y_i^{(r_i)}}{\partial u_i}\right|>0\Rightarrow\left|\beta_i\left(\hat{\boldsymbol{y}}_1,\boldsymbol{x}_2\right)\right|>\frac{1}{2}\left|\frac{\partial\alpha_i^1}{\partial u_i}+\beta_i\left(\boldsymbol{y}_1,\boldsymbol{x}_2\right)\right|>0\end{aligned} \tag{42}$$

The first condition in (42) implies that the estimated and actual control effectiveness have the same sign, and the second condition places a lower bound on the magnitude of the estimated control effectiveness.

Since the ideal NN weight vector $\boldsymbol{W}_{c,i}$ in (40) is unknown, the i^{th} controller NN output is given by

$$\nu_{ad,i}=\hat{\boldsymbol{W}}_{c,i}^T\left(t\right)\boldsymbol{\sigma}_c\left(\bar{\boldsymbol{\mu}}_c\right) \tag{43}$$

where $\hat{\boldsymbol{W}}_{c,i}\left(t\right)$ is an estimate for $\boldsymbol{W}_{c,i}$ that is updated online with the following adaptive law:

$$\dot{\hat{\boldsymbol{W}}}_{c,i}=-\Gamma_{c,i}\left(\boldsymbol{\sigma}_c\left(\bar{\boldsymbol{\mu}}_c\right)\hat{\boldsymbol{E}}_i^TP_{E,i}\bar{B}_{E,i}+\lambda_{c,i}\hat{\boldsymbol{W}}_{c,i}\right) \tag{44}$$

where $\Gamma_{c,i}>0$ is the NN adaptation gain and $\lambda_{c,i}>0$ is the sigma-mod parameter.

V. Lyapunov-like Stability Analysis

The boundedness of the integrated adaptive estimator and adaptive controller system is now shown via Lyapunov-like analysis. We consider the error analysis with respect to only the i^{th} regulated output y_i for convenience. Before starting the boundedness analysis, a few results are presented in the forms that are directly used in the analysis.

Define the state estimation error $\tilde{\boldsymbol{x}}_1 = \boldsymbol{x}_1 - \hat{\boldsymbol{x}}_1$, the observer NN weight estimation error $\tilde{\boldsymbol{W}}_{o,i}(t) = \boldsymbol{W}_{o,i} - \hat{\boldsymbol{W}}_{o,i}(t)$, the controller NN weight estimation error $\tilde{\boldsymbol{W}}_{c,i} = \boldsymbol{W}_{c,i} - \hat{\boldsymbol{W}}_{c,i}$ and $\bar{A}_1(t) = A_1 - K_1(t)C_1$. Using Eqs. (11) and (12), the state estimation error dynamics can be written as

$$\begin{aligned} \dot{\tilde{\boldsymbol{x}}}_1(t) &= \bar{A}_1(t)\tilde{\boldsymbol{x}}_1(t) + \sum_i^m \boldsymbol{b}_i \tilde{\boldsymbol{W}}_{o,i}^{\ T}(t)\boldsymbol{\sigma}_o(\bar{\boldsymbol{\mu}}_o) + \sum_i^m \boldsymbol{b}_i \varepsilon_{o,i}^{'}(\bar{\boldsymbol{\mu}}_o), \qquad \tilde{\boldsymbol{x}}_1(t_0) = \tilde{\boldsymbol{x}}_{10} \\ \tilde{\boldsymbol{y}}_1(t) &= C_1\tilde{\boldsymbol{x}}_1(t) \end{aligned} \tag{45}$$

The NN weight estimation error dynamics can be written using (25) as,

$$\dot{\tilde{\boldsymbol{W}}}_{o,i} = -\dot{\hat{\boldsymbol{W}}}_{o,i} = \Gamma_{o_i}\left(-\boldsymbol{\sigma}_o(\bar{\boldsymbol{\mu}}_o)C_{1,i}\tilde{\boldsymbol{x}}_1 - Q_{fi}^T\boldsymbol{e}_{na,1} + \lambda_o\boldsymbol{W}_{o,i} - \lambda_o\tilde{\boldsymbol{W}}_{o,i}\right) \tag{46}$$

Using the identity $P_1(t)P_1(t)^{-1} = I$ and differentiating, we have:

$$\begin{aligned} \dot{P}_1^{-1}(t) &= -P_1^{-1}(t)\bar{A}_1(t) - \bar{A}_1(t)^T P_1^{-1}(t) - \tilde{Q}_1(t) \\ \tilde{Q}_1(t) &= C^T R_1^{-1} C + P_1^{-1}(t) Q_1 P_1^{-1}(t) > 0 \end{aligned} \tag{47}$$

Since $P_1(t)$ is bounded, symmetric and positive definite, the following bounds on $P_1^{-1}(t)$ are used in the analysis [28],

$$\rho_1 I \le P_1(t) \le \rho_2 I \Rightarrow \frac{1}{\rho_2} I \le P_1^{-1}(t) \le \frac{1}{\rho_2} I \tag{48}$$

The second error signal used to train the NN can be re-written using Eqs. (21) and (24) as

$$\boldsymbol{e}_{na,1}(t) = T_1\left(\tilde{\boldsymbol{x}}_{na,1}(t_0), \varepsilon_{f1}^{'}, \varepsilon_{f2}^{'}, \cdots, \varepsilon_{fm}^{'}\right) + \sum_i^m Q_{fi}\tilde{\boldsymbol{W}}_{o,i} \tag{49}$$

Substituting (43) into Eqs. (36) and (39), we have:

$$\begin{aligned} \dot{\boldsymbol{E}}_i &= \bar{A}_{E,i}\boldsymbol{E}_i + \bar{B}_{E,i}\left(-\tilde{\boldsymbol{W}}_{c,i}^T\boldsymbol{\sigma}_c(\bar{\boldsymbol{\mu}}_c) - \varepsilon_{c,i}(\bar{\boldsymbol{\mu}}_c)\right) \\ \dot{\tilde{\boldsymbol{E}}}_i &= \tilde{A}_{E,i}\tilde{\boldsymbol{E}}_i + \bar{B}_{E,i}\left(-\tilde{\boldsymbol{W}}_{c,i}^T\boldsymbol{\sigma}_c(\bar{\boldsymbol{\mu}}_c) - \varepsilon_{c,i}(\bar{\boldsymbol{\mu}}_c)\right) \end{aligned} \tag{50}$$

Since $\tilde{A}_{E,i}$ is Hurwitz, then for any $\tilde{Q}_{E,i} > 0$, there exists a unique solution $\tilde{P}_{E,i} = \tilde{P}_{E,i}^T > 0$ of the following Lyapunov equation:

$$\tilde{A}_{E,i}^T\tilde{P}_{E,i} + \tilde{P}_{E,i}\tilde{A}_{E,i} = -\tilde{Q}_{E,i}, \quad \tilde{Q}_{E,i} = \tilde{Q}_{E,i}^T > 0 \tag{51}$$

The controller NN weight estimation error dynamics can be written using Eq. (44) as:

$$\dot{\tilde{\boldsymbol{W}}}_{c,i} = -\dot{\hat{\boldsymbol{W}}}_{c,i} = \Gamma_{c,i}\left\{\boldsymbol{\sigma}_c\left(\bar{\boldsymbol{\mu}}_c\right)\hat{\boldsymbol{E}}_i^T P_{E,i}\bar{B}_{E,i} + \lambda_{c,i}\left[\boldsymbol{W}_{c,i} - \tilde{\boldsymbol{W}}_{c,i}\right]\right\} \tag{52}$$

Define the composite error vector of the closed-loop system as

$$\boldsymbol{\zeta} = \begin{bmatrix}\boldsymbol{\zeta}_o^T & \boldsymbol{\zeta}_c^T\end{bmatrix}^T,\ \boldsymbol{\zeta}_o = \begin{bmatrix}\tilde{\boldsymbol{x}}_1^T & \tilde{\boldsymbol{W}}_{o,1}^T & \tilde{\boldsymbol{W}}_{o,2}^T & \cdots & \tilde{\boldsymbol{W}}_{o,m}^T\end{bmatrix}^T,\ \boldsymbol{\zeta}_c = \begin{bmatrix}\boldsymbol{E}_i^T, & \tilde{\boldsymbol{E}}_i^T, & \tilde{\boldsymbol{W}}_{c,i}^T\end{bmatrix}^T \tag{53}$$

and the positive definite candidate Lyapunov function for the boundedness analysis as

$$V\left(\boldsymbol{\zeta}\right) = V_o\left(\boldsymbol{\zeta}_o\right) + V_c\left(\boldsymbol{\zeta}_c\right),\ V_o\left(\boldsymbol{\zeta}_o\right) = \tilde{\boldsymbol{x}}_1^T P_1^{-1}\left(t\right)\tilde{\boldsymbol{x}}_1 + \sum_i^m \tilde{\boldsymbol{W}}_{o,i}^T \Gamma_{o_i}^{-1}\tilde{\boldsymbol{W}}_{o,i},\ V_c\left(\boldsymbol{\zeta}_c\right) = \boldsymbol{E}_i^T P_{E,i}\boldsymbol{E}_i + \tilde{\boldsymbol{E}}_i^T \tilde{P}_{E,i}\tilde{\boldsymbol{E}}_i + \tilde{\boldsymbol{W}}_{c,i}^T \Gamma_{c_i}^{-1}\tilde{\boldsymbol{W}}_{c,i} \tag{54}$$

Remark 4: The NN approximation for the modeling error functions in Eqs. (9) and (40) are defined over a compact sets D_g and D_{g_1}. In a combined estimation and control problem, since the boundedness of the states is not assured *a priori*, an assumption that the initial errors belong to a Lyapunov level set such that the input variables to the NNs lie within the compact sets defined in Eqs. (9) and (40), is one way to ensure that the NN approximations are valid. This is the basis for the next statement.

In the space of the error vector $\boldsymbol{\zeta}$, consider the largest level set of $V\left(\boldsymbol{\zeta}\right)$ such that its projection on the subspace of the NN input variables lies completely in D_g and D_{g_1}. Define the largest ball that lies within that level set as $B_{M_I} \triangleq \left\{\boldsymbol{\zeta} :\ \left\|\boldsymbol{\zeta}\right\| \le M_I\right\}$, where the subscript '*I*' is used to indicate that we are considering the integrated system, and let α_I be the minimum value of $V\left(\boldsymbol{\zeta}\right)$ on the boundary of B_{M_I}:

$$\alpha_I \triangleq \min_{\left\|\boldsymbol{\zeta}\right\| = M_I} V\left(\boldsymbol{\zeta}\right) \tag{55}$$

Introduce the set

$$\Omega_{\alpha_I} = \left\{\boldsymbol{\zeta} \in B_{M_I} \mid\ V\left(\boldsymbol{\zeta}\right) \le \alpha_I\right\} \tag{56}$$

Definition 1[1]: A continuous function $\alpha : [0, a) \mapsto \Re^+$ belongs to class K if it is strictly increasing and $\alpha\left(0\right) = 0$. It belongs to class K_∞ if $a = \infty$ and $\alpha\left(r\right) \to \infty$ as $r \to \infty$.

The definition of the candidate Lyapunov function (54) shows that there exist class K functions κ_3 and κ_4 such that

$$\kappa_3\left(\left\|\boldsymbol{\zeta}\right\|\right) \le V\left(\boldsymbol{\zeta}\right) \le \kappa_4\left(\left\|\boldsymbol{\zeta}\right\|\right)$$

$$\begin{aligned}
\kappa_3\left(\left\|\boldsymbol{\zeta}\right\|\right) &= \frac{1}{\rho_2^2}\left\|\tilde{\boldsymbol{x}}_1\right\|^2 + \sum_i^m \lambda_{\min}\left(\Gamma_{o,i}^{-1}\right)\left\|\tilde{\boldsymbol{W}}_{o,i}\right\|^2 + \lambda_{\min}\left(P_{E,i}\right)\left\|\boldsymbol{E}_i\right\|^2 + \lambda_{\min}\left(\tilde{P}_{E,i}\right)\left\|\tilde{\boldsymbol{E}}_i\right\|^2 + \lambda_{\min}\left(\Gamma_{c_i}^{-1}\right)\left\|\tilde{\boldsymbol{W}}_{c,i}\right\|^2 \\
\kappa_4\left(\left\|\boldsymbol{\zeta}\right\|\right) &= \frac{1}{\rho_1^2}\left\|\tilde{\boldsymbol{x}}_1\right\|^2 + \sum_i^m \lambda_{\max}\left(\Gamma_{o,i}^{-1}\right)\left\|\tilde{\boldsymbol{W}}_{o,i}\right\|^2 + \lambda_{\max}\left(P_{E,i}\right)\left\|\boldsymbol{E}_i\right\|^2 + \lambda_{\max}\left(\tilde{P}_{E,i}\right)\left\|\tilde{\boldsymbol{E}}_i\right\|^2 + \lambda_{\max}\left(\Gamma_{c_i}^{-1}\right)\left\|\tilde{\boldsymbol{W}}_{c,i}\right\|^2
\end{aligned} \tag{57}$$

where the bounds on $P_1^{-1}\left(t\right)$ in (48) are applied.

Assumption 7: Let

$$M_I > \kappa_3^{-1}\left(\kappa_4\left(\gamma_I\right)\right) \tag{58}$$

where γ_I is defined as

$$\gamma_I \triangleq \frac{\sqrt{\sum_j^m \left\{m_{1_j}^2 + m_{4_j}^2 + \lambda_o W_o^{*2}\right\} + l_1^2 + l_2^2 + \lambda_{c,i} W_c^{*2}}}{\min_{i=1,2,\cdots,m}\left(\sqrt{\frac{\lambda_{\min}\left(Q_1\right)}{\rho_2^2} - 2m}, \sqrt{\lambda_o - \left(m_{2_j}^2 + 2\right)}, \sqrt{\lambda_{\min}\left(Q_{E,i}\right) - 1}, \sqrt{\lambda_{\min}\left(\tilde{Q}_{E,i}\right) - 2}, \sqrt{\lambda_{c,i} - l_4^2}\right)}, \tag{59}$$

where:

$$\begin{aligned}
m_{1_i} &= \left\|P_1^{-1}(t)\boldsymbol{b}_i\right\|\varepsilon_o^* \\
m_{2_i} &= \left\|P_1^{-1}(t)\boldsymbol{b}_i - C_{1,i}^T\right\|\sqrt{N_o} \\
m_{4_i} &= \left\|Q_{fi}\right\|_F \left\|T_1\left(\tilde{\boldsymbol{x}}_{na,1}(t_0), \varepsilon_{f1}^{'}, \varepsilon_{f2}^{'}, \cdots, \varepsilon_{fm}^{'}\right)\right\| \\
l_1 &= \left\|\tilde{P}_{E,i}\bar{B}_{E,i}\right\|\varepsilon_c^* \\
l_2 &= \left\|P_{E,i}\bar{B}_{E,i}\right\|\varepsilon_c^* \\
l_4 &= \left\|P_{E,i}\bar{B}_{E,i} + \tilde{P}_{E,i}\bar{B}_{E,i}\right\|\sqrt{N_c}
\end{aligned} \tag{60}$$

Let $\lambda_{\min}\left(Q_1\right) > 2m\rho_2^2$ and $\lambda_o > \max\left\{m_{2_1}^2 + 2, m_{2_2}^2 + 2, \cdots, m_{2_m}^2 + 2\right\}$, $\lambda_{\min}\left(Q_{E,i}\right) > 1$, $\lambda_{\min}\left(\tilde{Q}_{E,i}\right) > 2$ and $\lambda_{c,i} > l_4^2$.

Now the main result on the error boundedness can be stated.

Theorem 2: Let Assumptions 1-7 hold and the initial error vector $\boldsymbol{\zeta}(t_0) \in \Omega_{\alpha_I}$. For the system formulation in (1) with the normal form given by (3), let the adaptive estimator be given by (12), the adaptive control law by (30), (31), the observer NN adaptive law by (25), and the controller NN adaptive law by (44). Then the closed-loop system errors $\boldsymbol{\zeta}$ are uniformly ultimately bounded.

Proof: Refer to Appendix.

VI. Application to Vision-based Formation Flight

The objective of the formation flight experiment will be for the follower aircraft to maintain a prescribed range from the leader aircraft in the presence of leader maneuvers and other unmodeled disturbances. No communication between the UAVs is assumed. The follower UAV is equipped with just one fixed camera for passive sensing of the LOS information.

The complete closed-loop system is summarized in the block diagram in Figure 1. The Image Processing and Computer Vision block takes as input the image frames from the onboard camera and processes them in real-time for visual tracking of a target (leader) aircraft. This block utilizes the method of *geometric active contours* [10,18] to track various features of interest in the image frames over a period of time. Active contours have the ability to conform to various object shapes and motions, making them ideal for segmentation, edge detection, shape modeling and visual tracking. Level set methods allow for fast, robust implementations of the algorithms for active contours algorithms [10,18]. For formation flight, the IGC block needs estimates of range and LOS angles between the leader and follower, and their derivatives. While the LOS angles are available from the images, the range is not. To estimate range from angle measurements, various implementations of an EKF are possible [10,17,19].

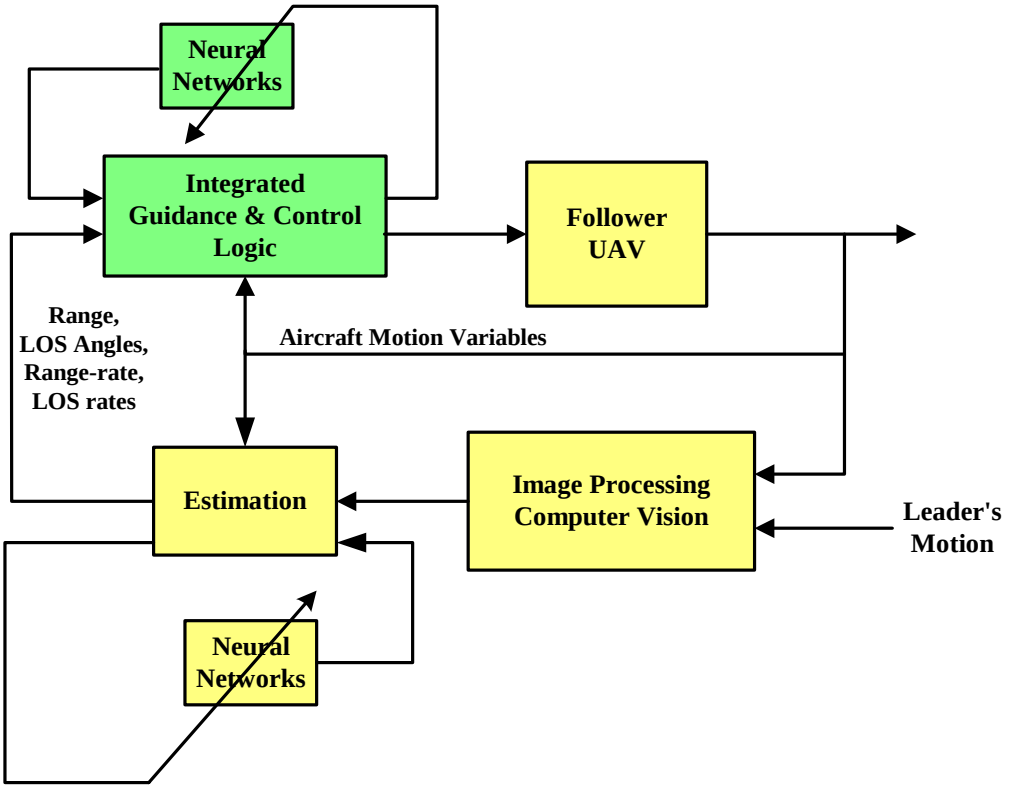

Figure 1. Closed-loop UAV System for LOS-based Formation Flight

A. Adaptive Target State Estimator

Consider the relative LOS kinematics between a leader and follower aircraft in the inertial Cartesian coordinate frame

$$\frac{d}{dt}\begin{bmatrix} R_X \\ \dot{R}_X \\ R_Y \\ \dot{R}_Y \\ R_Z \\ \dot{R}_Z \end{bmatrix} = \underbrace{\begin{bmatrix} 0 & 1 & 0 & 0 & 0 & 0 \\ 0 & 0 & 0 & 0 & 0 & 0 \\ 0 & 0 & 0 & 1 & 0 & 0 \\ 0 & 0 & 0 & 0 & 0 & 0 \\ 0 & 0 & 0 & 0 & 0 & 1 \\ 0 & 0 & 0 & 0 & 0 & 0 \end{bmatrix}}_{A} \begin{bmatrix} R_X \\ \dot{R}_X \\ R_Y \\ \dot{R}_Y \\ R_Z \\ \dot{R}_Z \end{bmatrix} + \underbrace{\begin{bmatrix} 0 & 0 & 0 \\ 1 & 0 & 0 \\ 0 & 0 & 0 \\ 0 & 1 & 0 \\ 0 & 0 & 0 \\ 0 & 0 & 1 \end{bmatrix}}_{B} \begin{bmatrix} a_{L_X} \\ a_{L_Y} \\ a_{L_Z} \end{bmatrix} + \begin{bmatrix} 0 & 0 & 0 \\ 1 & 0 & 0 \\ 0 & 0 & 0 \\ 0 & 1 & 0 \\ 0 & 0 & 0 \\ 0 & 0 & 1 \end{bmatrix} \begin{bmatrix} -a_{F_X} \\ -a_{F_Y} \\ -a_{F_Z} \end{bmatrix} \tag{61}$$

where R_X, R_Y and R_Z are respectively the projections of the range vector from the follower to the target aircraft onto the inertial X, Y and Z axes, and the subscripts *L* and *F* refer to leader and follower aircraft respectively. We assume that there is a vision sensor onboard the follower aircraft that can measure the subtended angle α, the azimuth angle λ_A, and the elevation angle λ_E with zero-mean additive measurement white noise of standard deviation 0.01 radians for each measurement. The subtended angle measures the maximum size subtended by the target aircraft on the follower image plane [19](see Figure 2). Using these raw noisy measurements, we can create pseudo-measurements of R_X, R_Y and R_Z using the relationship between α, λ_A, λ_E and assuming the leader wing-span size b is known:

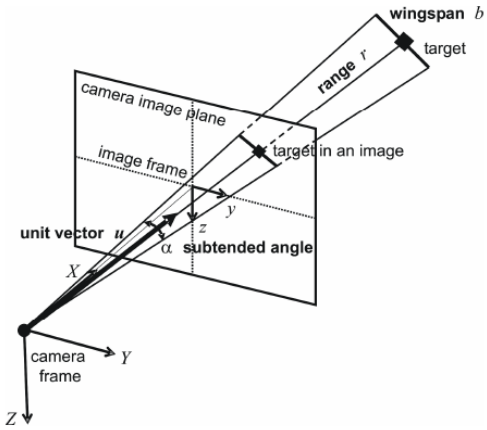

Figure 2. Image Plane Measurements of Target Aircraft

$$
\begin{aligned}
R_m &= \frac{b}{2\tan\left(\frac{\alpha_m}{2}\right)} \\
R_{X_m} &= R_m \cos\left(\lambda_{A_m}\right)\cos\left(\lambda_{E_m}\right) \\
R_{Y_m} &= R_m \sin\left(\lambda_{A_m}\right)\cos\left(\lambda_{E_m}\right) \\
R_{Z_m} &= -R_m \sin\left(\lambda_{E_m}\right)
\end{aligned}
\tag{62}
$$

where the subscript '*m*' is used to identify the variables in (62) as measurements. Eqs. (61) and (62) are used to design a linear time-varying Kalman filter as the nominal leader state estimator where the leader acceleration components along the inertial X, Y and Z axes are modeled as independent, zero-mean white noise processes. This filter is augmented by the output of an adaptive NN that is trained online using the composite adaptation law as discussed in Section III. The NN output generates estimates of the leader acceleration along the three coordinate axes to compensate the Kalman filter.

B. Adaptive Integrated Guidance and Control (IGC) Design for LOS Formation Flight

The objective of the control law design is for the follower aircraft to maintain a prescribed range to the leader aircraft in the presence of leader maneuvers while maintaining turn coordination. An IGC design does not require a time-scale separation assumption as is implicit in conventional outer-loop guidance and inner-loop autopilot designs. Hence an IGC design can achieve higher bandwidth for the combined guidance and flight control dynamics. An adaptive IGC design for a leader-follower LOS formation flight is discussed below. In the interest of keeping the paper length as short as possible, we are summarizing the control design and referring the derivations and other details to Ref. [3].

In the IGC formulation, the output variables to be regulated are chosen as $\left[R,\ \dot{\lambda}_A - \dot{\Psi},\ \dot{\lambda}_E - \dot{\Theta},\ a_{F_{Y_B}}\right]^T$, where R is the range, λ_A is the LOS azimuth with respect to the inertial X-axis, λ_E is the LOS elevation from the inertial horizontal plane, $\left[\Psi,\ \Theta,\ \Phi\right]^T$ represent the Euler attitude angles and $a_{F_{Y_B}}$ is the lateral acceleration, i.e., the specific force along the Y-axis of the body fixed frame. The lateral acceleration is regulated to zero to maintain turn coordination during maneuvers. The range command is given by a constant value, which is chosen as the length oftwo wing spans in the examples that follow. The variables $\chi_A \equiv \lambda_A - \Psi$ and $\chi_E \equiv \lambda_E - \Theta$ represent the bearing angles in the inertial coordinate frame. These angles are computable from the body attitude and LOS measurements obtained from an onboard camera fixed to the body of the follower aircraft, with the optical axis of the camera

coincident with the body x-axis. The bearing angle rate commands are set to zero. The bearing angles are not regulated since it is not desirable to restrict the follower aircraft to a particular relative position with respect to the leader aircraft, particularly in the presence of leader maneuvers. The range, elevation bearing rate, and turn coordination controllers are implemented via approximate feedback linearization augmented with the output of adaptive NNs, whereas the azimuth bearing rate controller is implemented via adaptive backstepping.

C. Simulation Results

A nonlinear 6-DOF simulation with linearized aerodynamics is used for the testing of the control and guidance algorithms for formation flight. Quaternion attitude angles are obtained by integrating the rate gyros. The simulation model is a rigid body aircraft model with 13 states, 3 for position with respect to the Earth-fixed frame, 3 for translational velocity expressed in the body frame, 4 for the quaternions and 3 for the angular velocity expressed in the body frame. Engine thrust is obtained from a linear interpolation map of throttle position. The actuators are modeled as first-order, stable linear filters with rate and position limits and time delays. The leader and follower aircraft are identical in their characteristics.

The range command is set to $R_{com} = 5$ meters, which is slightly less than 2 wing-span lengths. The wing-span length of the simulated aircraft is $b = 2.8$ meters. The commanded speed of the leader aircraft is $V_{com} = 25$ meters/sec. Noisy vision sensor measurements are simulated. We consider two leader maneuvers to evaluate the feasibility of the integrated estimation, guidance and control law.

Maneuver 1: Leader Maneuver in X-Z plane

Figure 3 shows the 2D trajectory of the leader and follower. Note that the Z-axis scale is magnified in comparison to the X axis. The leader aircraft tracks waypoints to generate the trajectory shown in the figure. The simulation is terminated once the leader aircraft reaches the last waypoint.

Figure 4 shows the range tracking performance with adaptation in the IGC design (NN_IGC = 1) and without adaptation. With adaptation, the range tracking error is bounded and goes towards the commanded value as the leader ends a maneuver. Without adaptation, the range tracking performance deteriorates as the leader aircraft maneuvers. The estimated range is also plotted in the figure. The range estimate almost coincides with the true range. This is to be expected since we have a reasonably accurate measurement of the range via the subtended angle, except at large ranges.

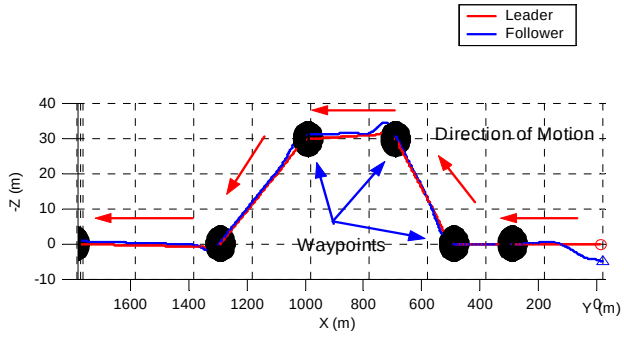

Figure 3. 2D Leader and Follower Trajectory, in meters (Maneuver 1)

Figure 5 plots the range-rate and elevation-rate estimates along side the true values. The subplots at the bottom of Figure 5a and b plot the estimation error. The peaks in the estimation error correspond to a leader climb or descent maneuver. These plots are for the case with adaptation.

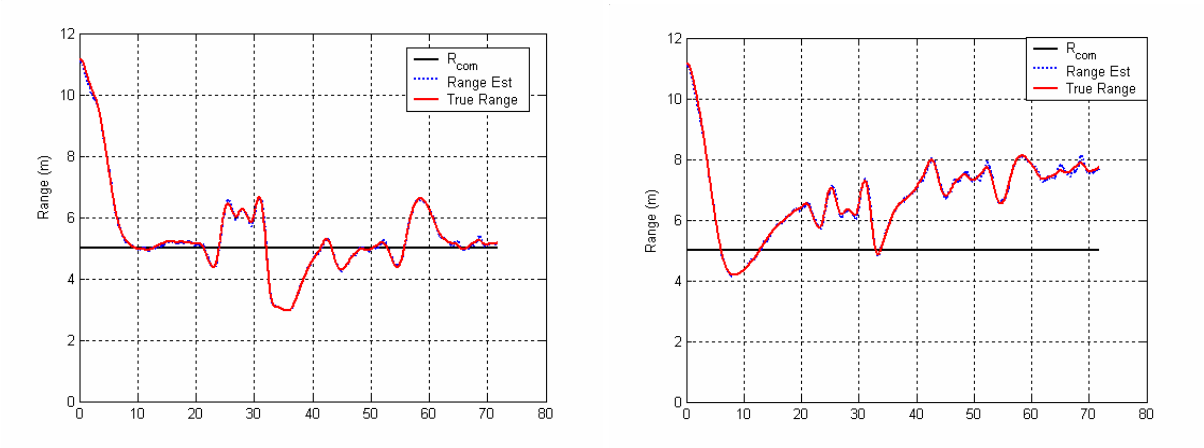

Figure 4. Range Tracking Performance, in ft (Maneuver 1), a) NN_IGC = 1, b) NN_IGC = 0

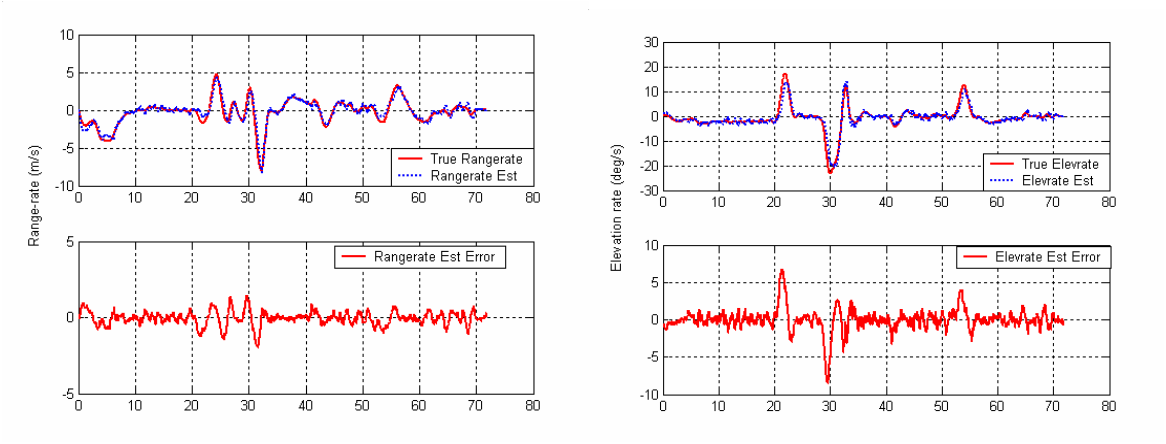

Figure 5. Estimation Performance (Maneuver 1), a) Range-rate Estimation (m/s), b) Elevation-rate Estimation (deg/s)

Maneuver 2: Leader Maneuver in 3D space

Figure 6 shows the trajectory of the formation for a maneuver in 3D space. In this maneuver, the leader aircraft starts at the origin and covers the first segment of the maneuver at constant velocity, then turns and climbs to the second waypoint, then turns at constant altitude to the third waypoint, and finally turns and descends to the starting position. This is a more severe maneuver compared to the preceding one.

Figure 7 compares the range tracking performance with and without adaptation in the IGC design and in the estimator design (NN_EKF = 1 and 0). With adaptation in both the IGC and estimation designs, the range tracking error is bounded and goes towards the commanded value as the leader ends a turning maneuver (Figure 7a). The estimated range is also plotted in the figure. It almost coincides with the true range. Without adaptation in the IGC design, the range tracking diverges and goes unstable as the leader aircraft maneuvers (Figure 7b). This happens in the first maneuver. The simulation was terminated once the range went to 25 meters. Without adaptation in estimation, there is clear deterioration in the range tracking and estimation performance as seen in Figure 7c.

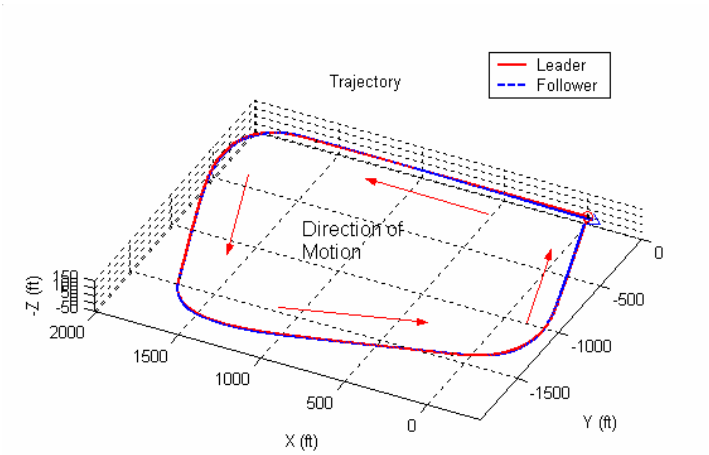

Figure 6. 3D Leader and Follower Trajectory, in ft (Maneuver 2)

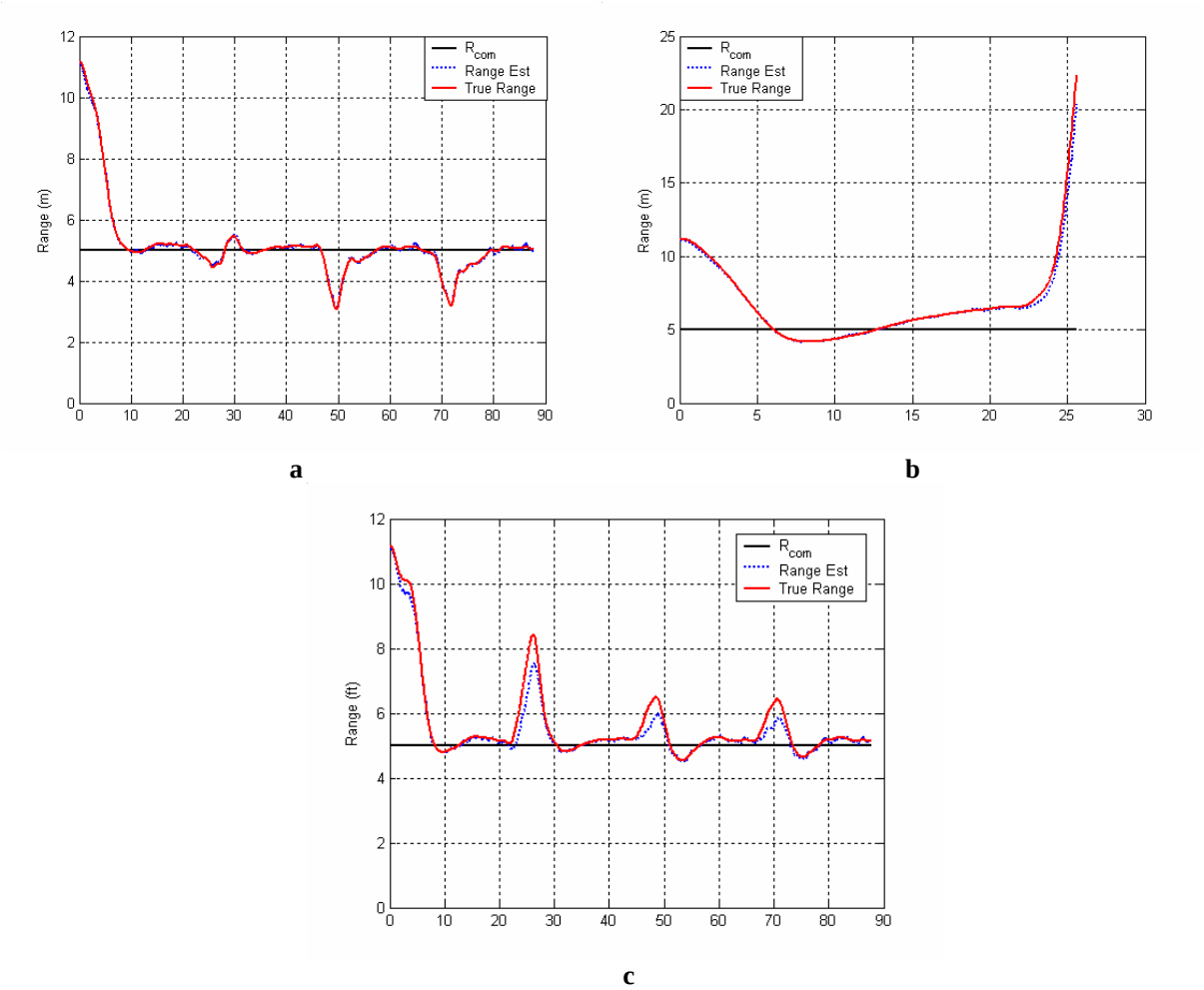

Figure 7. Range Tracking Performance, in meters (Maneuver 2), a) NN_IGC = 1 & NN_EKF =1, b) NN_IGC = 0 & NN_EKF =1, c) NN_IGC = 1 & NN_EKF = 0

Figure 8 plots the leader aircraft acceleration in the inertial 3D coordinates along with the corresponding estimates that are generated by the adaptive NN augmenting the Kalman filter. The observer NN estimates the true leader acceleration with a slight lag.

Figure 9 plots the actuator histories for the follower aircraft with adaptation in the IGC and estimator designs. The actuator deflections are moderate with some oscillations in the aileron and rudder channels due to the effect of measurement noise.

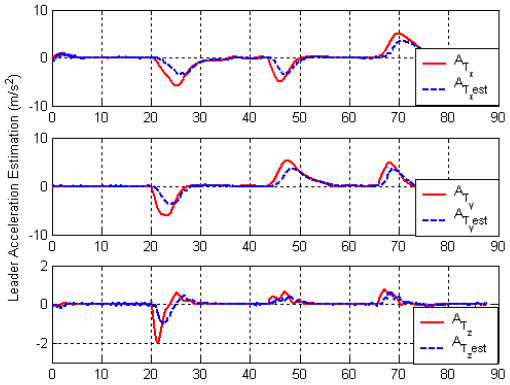

Figure 8. Leader Acceleration Estimation, in m/s^2 (Maneuver 2)

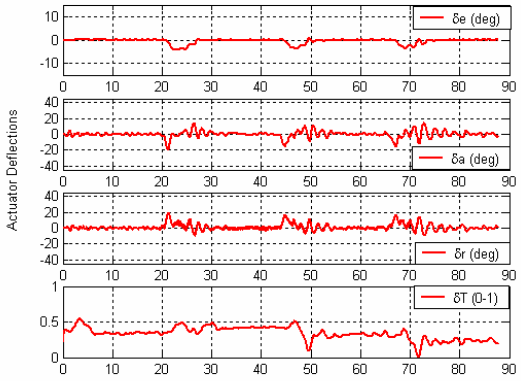

Figure 9. Actuator Histories (Maneuver 2)

Future research will involve integrating the presented adaptive estimation, guidance and control law with a vision sensor and image processing algorithms and flight test the overall architecture.

VII. Conclusions

In this paper we have presented a method to integrate adaptive estimation and adaptive control designs for a class of nonlinear systems with unmodeled dynamics. The method is based on Lyapunov-like stability analysis of all the errors in the integrated closed-loop system. The presented approach is then implemented in a vision-based formation flight control problem. Integration of the adaptive estimator and the adaptive IGC design makes the vision-based formation control design practical. Simulation results using nonlinear 6DOF fixed-wing UAV models show that adaptation in both the estimation and integrated guidance and control (IGC) designs is critical to the stability and performance of the range tracking performance.

Appendix A: Proof of Lemma 1

We prove GES of the dynamics in (19) via Lyapunov stability analysis. First we derive Eqs. (A-1)-(A-2) that are used in the analysis. The matrix differential equation (16) can be re-written as

$$\dot{P}_{na,1}(t) = \bar{A}_{na,1}(t) P_{na,1}(t) + P_{na,1}(t) \bar{A}_{na,1}(t)^T + P_{na,1}(t) C_1^T R_{na,1}^{-1} C_1 P_{na,1}(t) + Q_{na,1} \tag{A-1}$$

Using $P_{na,1}(t) P_{na,1}(t)^{-1} = I$ and differentiating, we have:

$$\begin{aligned} \dot{P}_{na,1}{}^{-1}(t) &= -P_{na,1}{}^{-1}(t) \bar{A}_{na,1}(t) - \bar{A}_{na,1}(t)^T P_{na,1}{}^{-1}(t) - \tilde{Q}_{na,1}(t) \\ \tilde{Q}_{na,1}(t) &= C_1^T R_{na,1}^{-1} C_1 + P_{na,1}{}^{-1}(t) Q_{na,1} P_{na,1}{}^{-1}(t) > 0 \end{aligned} \tag{A-2}$$

Now consider the Lyapunov candidate function $V_1(t, \tilde{\boldsymbol{x}}_{na,1}) = \tilde{\boldsymbol{x}}_{na,1}^T P_{na,1}{}^{-1}(t) \tilde{\boldsymbol{x}}_{na,1}$. Since $P_{na,1}(t)$ is bounded, symmetric and positive definite, there exist positive constants ρ_3 and ρ_4, $\rho_3 > \rho_4 > 0$, such that

$$0 < \frac{1}{\rho_3} \left\| \tilde{\boldsymbol{x}}_{na,1} \right\|^2 \le V_1(t, \tilde{\boldsymbol{x}}_{na,1}) \le \frac{1}{\rho_4} \left\| \tilde{\boldsymbol{x}}_{na,1} \right\|^2 \tag{A-3}$$

So $V_1(t, \tilde{\boldsymbol{x}}_{na,1})$ is decresent and radially unbounded [1]. Differentiating $V_1(t, \tilde{\boldsymbol{x}}_{na,1})$

$$\dot{V}_1(t, \tilde{\boldsymbol{x}}_{na,1}) = \dot{\tilde{\boldsymbol{x}}}_{na,1}^T P_{na,1}(t)^{-1} \tilde{\boldsymbol{x}}_{na,1} + \tilde{\boldsymbol{x}}_{na,1}^T P_{na,1}(t)^{-1} \dot{\tilde{\boldsymbol{x}}}_{na,1} + \tilde{\boldsymbol{x}}_{na,1}^T \dot{P}_{na,1}(t)^{-1} \tilde{\boldsymbol{x}}_{na,1} \tag{A-4}$$

Substituting for $\dot{\tilde{\boldsymbol{x}}}_{na,1}$ from (19) and $\dot{P}_{na,1}{}^{-1}(t)$ from (A-2), Eq. (A-4)simplifies to

$$\dot{V}_1(t, \tilde{\boldsymbol{x}}_{na,1}) = -\tilde{\boldsymbol{x}}_{na,1}^T \tilde{Q}_{na,1}(t) \tilde{\boldsymbol{x}}_{na,1} \le -\lambda_{\min}\left(\tilde{Q}_{na,1}(t)\right) \left\| \tilde{\boldsymbol{x}}_{na,1} \right\|^2 \tag{A-5}$$

By Corollary 3.4, pp. 140 in Ref. [1], the $\tilde{\boldsymbol{x}}_{na,1} \equiv 0$ is GES. The time-domain solution of (19) is given by

$$\tilde{\boldsymbol{x}}_{na,1}(t) = \Phi_{na,1}(t, t_0) \tilde{\boldsymbol{x}}_{na,1}(t_0), \quad \forall t \ge t_0 \ge 0 \tag{A-6}$$

By definition of GES for non-autonomous systems [1],

$$\left\| \tilde{\boldsymbol{x}}_{na,1}(t) \right\| = \left\| \Phi_{na,1}(t, t_0) \tilde{\boldsymbol{x}}_{na,1}(t_0) \right\| \le k \left\| \tilde{\boldsymbol{x}}_{na,1}(t_0) \right\| e^{-\lambda(t - t_0)} \tag{A-7}$$

for some positive constants k and λ and for all $\tilde{\boldsymbol{x}}_{na,1}(t_0) \in R^{n_1}$. This implies that

$$\Phi_{na,1}(t, t_0) \tilde{\boldsymbol{x}}_{na,1}(t_0) \to 0, \text{ as } t \to \infty \tag{A-8}$$

Since the estimation error dynamics in (19) are GES, in the presence of the bounded input $\boldsymbol{g}(\boldsymbol{x}_1, \boldsymbol{z})$ the estimation error vector $\tilde{\boldsymbol{x}}_{na,1}$ of the system is input-to-state stable [1]. This implies that $\tilde{\boldsymbol{x}}_{na,1}(t)$ is bounded as long as $\boldsymbol{g}(\boldsymbol{x}_1, \boldsymbol{z})$ is bounded. This also implies that the residual $\tilde{\boldsymbol{y}}_{na,1}(t)$ is bounded as long as $\boldsymbol{g}(\boldsymbol{x}_1, \boldsymbol{z})$ is bounded.

□

Appendix B: Proof of Theorem 2

Differentiating the Lyapunov candidate function $V(\boldsymbol{\zeta})$ defined in (54):

$$\dot{V}(\boldsymbol{\zeta}) = \dot{V}_o(\boldsymbol{\zeta}_o) + \dot{V}_c(\boldsymbol{\zeta}_c) \tag{B-1}$$

$$\begin{aligned} \dot{V}_o(\boldsymbol{\zeta}_o) &= \dot{\tilde{\boldsymbol{x}}}_1^T P_1^{-1}(t)\tilde{\boldsymbol{x}}_1 + \tilde{\boldsymbol{x}}_1^T P_1^{-1}(t)\dot{\tilde{\boldsymbol{x}}}_1 + \tilde{\boldsymbol{x}}_1^T \dot{P}_1^{-1}(t)\tilde{\boldsymbol{x}}_1 + 2\sum_i^m \tilde{\boldsymbol{W}}_{o,i}^T \Gamma_{o_i}^{-1} \dot{\tilde{\boldsymbol{W}}}_{o,i} \\ \dot{V}_c(\boldsymbol{\zeta}_c) &= \dot{\boldsymbol{E}}_i^T P_{E,i}\boldsymbol{E}_i + \boldsymbol{E}_i^T P_{E,i}\dot{\boldsymbol{E}}_i + \dot{\tilde{\boldsymbol{E}}}_i^T \tilde{P}_{E,i}\tilde{\boldsymbol{E}}_i + \tilde{\boldsymbol{E}}_i^T \tilde{P}_{E,i}\dot{\tilde{\boldsymbol{E}}}_i + 2\tilde{\boldsymbol{W}}_{c,i}^T \Gamma_{c_i}^{-1}\dot{\tilde{\boldsymbol{W}}}_{c,i} \end{aligned} \tag{B-2}$$

Substituting Eqs. (45), (46), (47), (50) into (B-2), substituting $\boldsymbol{E}_i = \hat{\boldsymbol{E}}_i + \tilde{\boldsymbol{E}}_i$ and simplifying, we have:

$$\begin{aligned} \dot{V}_o(\boldsymbol{\zeta}_o) &= -\tilde{\boldsymbol{x}}_1^T \tilde{Q}_1(t)\tilde{\boldsymbol{x}}_1 + 2\tilde{\boldsymbol{x}}_1^T \sum_i^m P_1^{-1}(t)\boldsymbol{b}_i \tilde{\boldsymbol{W}}_{o,i}^T \boldsymbol{\sigma}_o(\bar{\boldsymbol{\mu}}_o) + 2\tilde{\boldsymbol{x}}_1^T \sum_i^m P_1^{-1}(t)\boldsymbol{b}_i \varepsilon_{o,i}'(\bar{\boldsymbol{\mu}}_o) \\ &\quad + 2\sum_i^m \tilde{\boldsymbol{W}}_{o,i}^T \left(-\boldsymbol{\sigma}_o(\bar{\boldsymbol{\mu}}_o) C_{1,i}\tilde{\boldsymbol{x}}_1 - Q_{fi}^T \boldsymbol{e}_{na,1}\right) + 2\lambda_o \sum_i^m \tilde{\boldsymbol{W}}_{o,i}^T \boldsymbol{W}_{o,i} - 2\lambda_o \sum_i^m \tilde{\boldsymbol{W}}_{o,i}^T \tilde{\boldsymbol{W}}_{o,i} \\ \dot{V}_c(\boldsymbol{\zeta}_c) &= -\boldsymbol{E}_i^T Q_{E,i}\boldsymbol{E}_i - \dot{\tilde{\boldsymbol{E}}}_i^T \tilde{Q}_{E,i}\tilde{\boldsymbol{E}}_i - 2\tilde{\boldsymbol{W}}_{c,i}^T \left(\boldsymbol{\sigma}_c \hat{\boldsymbol{E}}_i^T P_{E,i}\bar{B}_{E,i} + \Gamma_{c_i}^{-1}\dot{\hat{\boldsymbol{W}}}_{c,i}\right) \\ &\quad - 2\tilde{\boldsymbol{E}}_i^T \left(P_{E,i}\bar{B}_{E,i} + \tilde{P}_{E,i}\bar{B}_{E,i}\right)\tilde{\boldsymbol{W}}_{c,i}^T \boldsymbol{\sigma}_c - 2\boldsymbol{E}_i^T P_{E,i}\bar{B}_{E,i}\varepsilon_c - 2\tilde{\boldsymbol{E}}_i^T \tilde{P}_{E,i}\bar{B}_{E,i}\varepsilon_c \end{aligned} \tag{B-3}$$

$\dot{V}_o$ can be upper-bounded using Eqs. (47)and (9) and $\dot{V}_c$ can be upper-bounded by substituting the adaptive control law in (44), using the identity $\|\boldsymbol{\sigma}_c\| \le \sqrt{N_c}$ and simplifying using Eq. (60),

$$\begin{aligned} \dot{V}_o &\le -\tilde{\boldsymbol{x}}_1^T P_1^{-1}(t) Q_1 P_1^{-1}(t)\tilde{\boldsymbol{x}}_1 + 2\tilde{\boldsymbol{x}}_1^T \sum_i^m P_1^{-1}(t)\boldsymbol{b}_i \tilde{\boldsymbol{W}}_{o,i}^T \boldsymbol{\sigma}_o(\bar{\boldsymbol{\mu}}_o) + 2\sum_i^m \|\tilde{\boldsymbol{x}}_1\| \|P_1^{-1}(t)\boldsymbol{b}_i\| \varepsilon_o^* \\ &\quad -2\tilde{\boldsymbol{x}}_1^T \sum_i^m C_{1,i}^T \tilde{\boldsymbol{W}}_{o,i}^T \boldsymbol{\sigma}_o(\bar{\boldsymbol{\mu}}_o) - 2\sum_i^m \tilde{\boldsymbol{W}}_{o,i}^T Q_{fi}^T \boldsymbol{e}_{na,1} + 2\lambda_o \sum_{\boldsymbol{i}}^{\boldsymbol{m}} \|\tilde{\boldsymbol{W}}_{o,i}\| W_o^* - 2\lambda_o \sum_i^m \|\tilde{\boldsymbol{W}}_{o,i}\|^2 \\ \dot{V}_c &\le -\lambda_{\min}(Q_{E,i}) \|\boldsymbol{E}_i\|^2 - \lambda_{\min}(\tilde{Q}_{E,i}) \|\tilde{\boldsymbol{E}}_i\|^2 - 2\lambda_{c,i} \|\tilde{\boldsymbol{W}}_{c,i}\|^2 + 2\lambda_{c,i} \tilde{\boldsymbol{W}}_{c,i}^T \boldsymbol{W}_{c,i} \\ &\quad + 2l_4 \|\tilde{\boldsymbol{E}}_i\| \|\tilde{\boldsymbol{W}}_{c,i}\| + 2l_2 \|\boldsymbol{E}_i\| + 2l_1 \|\tilde{\boldsymbol{E}}_i\| \end{aligned} \tag{B-4}$$

Combining terms and expanding the expression for $\boldsymbol{e}_{na,1}$ using (49),

$$\begin{aligned} \dot{V}_o &\le -\tilde{\boldsymbol{x}}_1^T P_1^{-1}(t) Q_1 P_1^{-1}(t)\tilde{\boldsymbol{x}}_1 - 2\lambda_o \sum_i^m \|\tilde{\boldsymbol{W}}_{o,i}\|^2 + 2\tilde{\boldsymbol{x}}_1^T \sum_i^m \left[P_1^{-1}(t)\boldsymbol{b}_i - C_{1,i}^T\right] \boldsymbol{\sigma}_o^T(\bar{\boldsymbol{\mu}}_o)\tilde{\boldsymbol{W}}_{o,i} + 2\sum_i^m \|\tilde{\boldsymbol{x}}_1\| \|P_1^{-1}(t)\boldsymbol{b}_i\| \varepsilon_o^* \\ &\quad -2\underbrace{\sum_i^m \tilde{\boldsymbol{W}}_{o,i}^T Q_{fi}^T \left(\sum_k^m Q_{fk}\tilde{\boldsymbol{W}}_{o,k}\right)}_{\ge 0} - 2\sum_i^m \tilde{\boldsymbol{W}}_{o,i}^T Q_{fi}^T T_1\left(\tilde{\boldsymbol{x}}_{na,1}(t_0), \varepsilon_{f1}', \varepsilon_{f2}', \cdots, \varepsilon_{fm}'\right) + 2\lambda_o \sum_{\boldsymbol{i}}^{\boldsymbol{m}} \|\tilde{\boldsymbol{W}}_{o,i}\| W_o^* \end{aligned} \tag{B-5}$$

The boundedness of $T_1\left(\tilde{\boldsymbol{x}}_{na,1}(t_0), \varepsilon_{f1}', \varepsilon_{f2}', \cdots, \varepsilon_{fm}'\right)$ and Q_{fi} in Eqs. (21) and (22) as a result of Lemma 1 is used in the definition of m_{4_i} in (60). Using the identity $\|\boldsymbol{\sigma}_o(\bar{\boldsymbol{\mu}}_o)\| \le \sqrt{N_o}$ and applying Eq. (60) in(B-5), $\|\boldsymbol{W}_{c,i}\| \le W_c^*$ in (B-4) , and completing squares,

$$\dot{V}_o \le -\frac{\lambda_{\min}\left(Q_1\right)}{\rho_2^2}\left\|\tilde{\boldsymbol{x}}_1\right\|^2 - 2\lambda_o\sum_i^m\left\|\tilde{\boldsymbol{W}}_{o,i}\right\|^2 + 2\sum_i^m m_{2_i}\left\|\tilde{\boldsymbol{x}}_1\right\|\left\|\tilde{\boldsymbol{W}}_{o,i}\right\| + 2\sum_i^m m_{1_i}\left\|\tilde{\boldsymbol{x}}_1\right\| + 2\sum_i^m m_{4_i}\left\|\tilde{\boldsymbol{W}}_{o,i}\right\| + \lambda_o\sum_i^m\left\|\tilde{\boldsymbol{W}}_{o,i}\right\|^2 + \lambda_o\sum_i^m W_o^{*^2}$$
$$\dot{V}_c \le -\left\|\boldsymbol{E}_i\right\|^2\left(\lambda_{\min}\left(Q_{E,i}\right)-1\right) - \left\|\tilde{\boldsymbol{E}}_i\right\|^2\left(\lambda_{\min}\left(\tilde{Q}_{E,i}\right)-2\right) - \left\|\tilde{\boldsymbol{W}}_{c,i}\right\|^2\left(\lambda_{c,i}-l_4^2\right) + l_1^2 + l_2^2 + \lambda_{c,i}W_c^{*^2} \tag{B-6}$$

Finally, completing squares in (B-6) and combining using (B-1),

$$\dot{V}\left(\boldsymbol{\zeta}\right) \le -\left\|\tilde{\boldsymbol{x}}_1\right\|^2\left(\frac{\lambda_{\min}\left(Q_1\right)}{\rho_2^2} - 2m\right) - \sum_i^m\left\|\tilde{\boldsymbol{W}}_{o,i}\right\|^2\left(\lambda_o - m_{2_i}^2 - 1\right) - \left\|\boldsymbol{E}_i\right\|^2\left(\lambda_{\min}\left(Q_{E,i}\right)-1\right) - \left\|\tilde{\boldsymbol{E}}_i\right\|^2\left(\lambda_{\min}\left(\tilde{Q}_{E,i}\right)-2\right)$$
$$-\left\|\tilde{\boldsymbol{W}}_{c,i}\right\|^2\left(\lambda_{c,i}-l_4^2\right) + \sum_i^m\left[m_{1_i}^2 + m_{4_i}^2 + \lambda_o W_o^{*^2}\right] + l_1^2 + l_2^2 + \lambda_{c,i}W_c^{*^2} \tag{B-7}$$

Thus either of the following conditions:

$$\left\|\tilde{\boldsymbol{x}}_1\right\| > \sqrt{\frac{\sum_i^m\left\{m_{1_i}^2 + m_{4_i}^2 + \lambda_o W_o^{*^2}\right\} + l_1^2 + l_2^2 + \lambda_{c,i}W_c^{*^2}}{\frac{\lambda_{\min}\left(Q_1\right)}{\rho_2^2} - 2m}} \tag{B-8}$$

$$\left\|\tilde{\boldsymbol{W}}_{o,i}\right\| > \sqrt{\frac{\sum_i^m\left\{m_{1_i}^2 + m_{4_i}^2 + \lambda_o W_o^{*^2}\right\} + l_1^2 + l_2^2 + \lambda_{c,i}W_c^{*^2}}{\lambda_o - \left(m_{2_i}^2 + 2\right)}}, \quad i = 1, 2, \cdots, m \tag{B-9}$$

$$\left\|\boldsymbol{E}_i\right\| > \sqrt{\frac{\sum_i^m\left\{m_{1_i}^2 + m_{4_i}^2 + \lambda_o W_o^{*^2}\right\} + l_1^2 + l_2^2 + \lambda_{c,i}W_c^{*^2}}{\lambda_{\min}\left(Q_{E,i}\right)-1}} \tag{B-10}$$

$$\left\|\tilde{\boldsymbol{E}}_i\right\| > \sqrt{\frac{\sum_i^m\left\{m_{1_i}^2 + m_{4_i}^2 + \lambda_o W_o^{*^2}\right\} + l_1^2 + l_2^2 + \lambda_{c,i}W_c^{*^2}}{\lambda_{\min}\left(\tilde{Q}_{E,i}\right)-2}} \tag{B-11}$$

$$\left\|\tilde{\boldsymbol{W}}_{c,i}\right\| > \sqrt{\frac{\sum_i^m\left\{m_{1_i}^2 + m_{4_i}^2 + \lambda_o W_o^{*^2}\right\} + l_1^2 + l_2^2 + \lambda_{c,i}W_c^{*^2}}{\lambda_{c,i} - l_4^2}} \tag{B-12}$$

will guarantee that $\dot{V}\left(\boldsymbol{\zeta}\right) < 0$ outside the compact set

$$B_{\gamma_I} = \left\{\boldsymbol{\zeta} \in B_{M_I} \mid \left\|\boldsymbol{\zeta}\right\| \le \gamma_I\right\} \tag{B-13}$$

Note that $B_{\gamma_I} \subset B_{M_I}$ from Eq. (58). Let β_I be the maximum value of the Lyapunov function $V\left(\boldsymbol{\zeta}\right)$ on the boundary of B_{γ_I}

$$\beta_I \triangleq \max_{\left\|\boldsymbol{\zeta}\right\|=\gamma_I} V\left(\boldsymbol{\zeta}\right) \tag{B-14}$$

Introduce the set

$$\Omega_{\beta_1} = \left\{ \zeta \mid V(\zeta) \leq \beta_1 \right\} \tag{B-15}$$

Eq. (58) ensures that $\Omega_{\beta_1} \subset \Omega_{\alpha_1}$ and thus ultimate boundedness of ζ with ultimate bound equal to $\kappa_3^{-1}\left(\kappa_4\left(\gamma_1\right)\right)$. □

Remark 5: The size of the ultimate bounds on the errors can be controlled by tuning the design parameters Q_1, $Q_{E,i}$, $\tilde{Q}_{E,i}$, λ_o and $\lambda_{c,i}$

Acknowledgments

This research has been sponsored under AFOSR contract F49620-03-1-0401.

References

[1] H.K. Khalil, *Nonlinear Systems*, 2nd Edition, Prentice Hall Inc., 1996.

[2] R. Sattigeri and A.J. Calise, "Neural Network Augmented Kalman Filtering in the Presence of Unknown System Inputs," *AIAA Guidance, Navigation, and Control Conference*, Keystone, CO, August 2006.

[3] Y.H. Kim and F.L. Lewis, "Neural Network Output Feedback Control of Robot Manipulators," *IEEE Transactions on Robotics and Automation,* Vol. 15, No. 2, pp. 301-309, April 1999.

[4] A. Isidori, "*Nonlinear Control Systems*", Springer-Verlag, Berlin, 1989.

[5] J.Y. Choi and J.A. Farrell, "Adaptive Observer Backstepping Control using Neural Networks," *IEEE Transactions on Neural Networks,* Vol. 12, No. 5, pp. 1103-1112, September 2001.

[6] L. Jiang and Q.H. Wu, "Nonlinear Adaptive Control via Sliding-Mode State and Perturbation Observer," *IEEE Proceedings on Control Theory Applications,* Vol. 149, No. 4, pp. 269-277, July 2002.

[7] Y. Wang and T. Chai, "Output Feedback Control of Uncertain Nonlinear Systems using Adaptive Fuzzy Observer," *American Control Conference,* pp. 2613-2618, June 2005.

[8] N. Hovakimyan, F. Nardi, A.J. Calise and H. Lee, "Adaptive Output Feedback Control of a Class of Nonlinear Systems using Neural Networks," *International Journal of Control,* Vol. 74, No. 12, pp. 1161-1169, 2001.

[9] N. Hovakimyan, R. Rysdyk and A.J. Calise, "Dynamic Neural Networks for Output Feedback Control," *Proc of the Conference on Decision and Control,* pp. 1685-1690, December 1999.

[10] A. Betser, P. Vela, and A. Tannenbaum, "Automatic Tracking of Flying Vehicles Using Geodesic snakes and Kalman filtering," *IEEE Conference on Decision and Control*, Vol. 2, pp 1649-1654, December 2004.

[11] L. Polloni, R. Mati, M. Innocenti, G. Campa and M. Napolitano, "A Synthetic Environment for the Simulation of Vision-based Formation Flight, " *AIAA Modeling and Simulation Technologies Conference*, Austin, Texas, August 2003.

[12] B.S. Kim, A. J. Calise, and R. Sattigeri, "Adaptive, Integrated Guidance and Control Design for Line-of-Sight based Formation Flight," *to appear in AIAA Journal of Guidance, Control and Dynamics*, 2007.

[13] P. K. Menon and E..J. Ohlmeyer, "Integrated Design of Agile Missile Guidance and Autopilot Systems," *IFAC – Control Engineering Practice*, Vol. 9, pp. 1095-1106, 2001.

[14] P. K. Menon, G. D. Sweriduk and E..J. Ohlmeyer, "Optimal Fixed-Interval Integrated Guidance-Control Laws for Hit-to-Kill Missiles," *AIAA Guidance, Navigation, and Control Conference*, Austin, TX, August 2003.

[15] I. Shkolnikov, Y. Shtessel, and D. Lianos, "Integrated Guidance-Control System of a Homing Interceptor - Sliding Mode Approach," *AIAA Guidance, Navigation, and Control Conference*, Montreal, Canada, August 2001.

[16] M. Sharma and N. Richards, "Adaptive, Integrated Guidance and Control for Missile Interceptors," *AIAA Guidance, Navigation, and Control Conference*, Providence, RI, August 2004.

[17] V.K. Madyastha and A.J. Calise, "An Adaptive Filtering Approach to Target Tracking", *American Control Conference,* pp. 1269-1274, June 2005.

[18] J. Ha, C. Alvino, G. Pryor, M. Niethammer, E. Johnson, and A. Tannenbaum, "Active Contours and Optical Flow for Automatic Tracking of Flying Vehicles," *American Control Conference*, Vol. 4, pp 3441-3446, 2004.

[19] E. Johnson, A. Calise, R. Sattigeri, Y. Watanabe, and V. Madyastha, "Approaches to Vision-based Formation Control," *IEEE Conference on Decision and Control*, Vol. 2, pp 1643-1648, December 2004.

[20] N. Hovakimyan, A.J. Calise and N. Kim, "Adaptive Output Feedback Control of a Class of Multi-Input Multi-Output Systems using Neural Networks," *International Journal of Control*, October 2004, vol. 77, no. 15, pp 1318-1329.

[21] R. G. Brown and P.Y.C. Hwang, *Introduction to Random Signals and Applied Kalman Filtering*, John Wiley and Sons Inc., 1992.

[22] E. Lavretsky, N. Hovakimyan and A.J. Calise, "Upper Bounds for Approximation of Continuous Time Dynamics using Delayed Outputs and Feedforward Neural Networks", *IEEE Transactions on Automatic Control,* AC-48, pp. 1606-1610, September 2003.
[23] K.S. Narendra and A.M. Annaswamy, "A New Adaptive Law for Robust Adaptation without Persistent Excitation", *IEEE Transactions on Automatic Control,* AC-32, pp. 134-145, 1987.
[24] B-J. Yang, N. Hovakimyan and A.J. Calise, "Output Feedback Control of an Uncertain System using an Adaptive Observer," *IEEE Conference on Decision and Control*, pp. 1705-1710, December 2003.
[25] A.J. Calise, N. Hovakimyan and M. Idan, "Adaptive Output Feedback Control of Nonlinear Systems Using Neural Networks," *Automatica*, 2001, vol. 37, no. 8, pp 1201-1211.
[26] Y. Kim and F. Lewis, *High Level Feedback Control with Neural Networks*, World Scientific, N.J., 1998.
[27] G. Cybenko, "Approximations by superpositions of sigmoidal function," *Mathematics, Control, Signals, Systems*, Vol. 2, pp. 303-314, 1989.
[28] V. Madyastha and A.J. Calise, "Adaptive Estimation for Control of Uncertain Nonlinear Systems with Applications to Target Intercept," *AIAA Guidance, Navigation, and Control Conference*, Keystone, CO, August 2006.